High-Z Detectors

Abdul K. Rumaiz

National Synchrotron Light Source II – Brookhaven National Laboratory

EDIT school 2023

Outline

- X-ray detector: Quick Recap
- Germanium for Synchrotron Science
  - ✓ Overview/background
  - ✓ Detector System
    - Sensor
    - ASIC (MARS)
  - ✓ Ge-strip Detectors for synchrotron science
  - ✓ New Ge Detectors: Ge drift detectors, GAIA, Gepta-EX…
- Amorphous Selenium for Medical Imaging
  - ✓ Overview/background
  - ✓ Preliminary results
    - High spatial resolution detector with CMOS readout
  - ✓ Proposed research
    - SWAD with High-k blocking layer
- Large band gap semiconductor (Diamond, CZT for Gamma rays…)

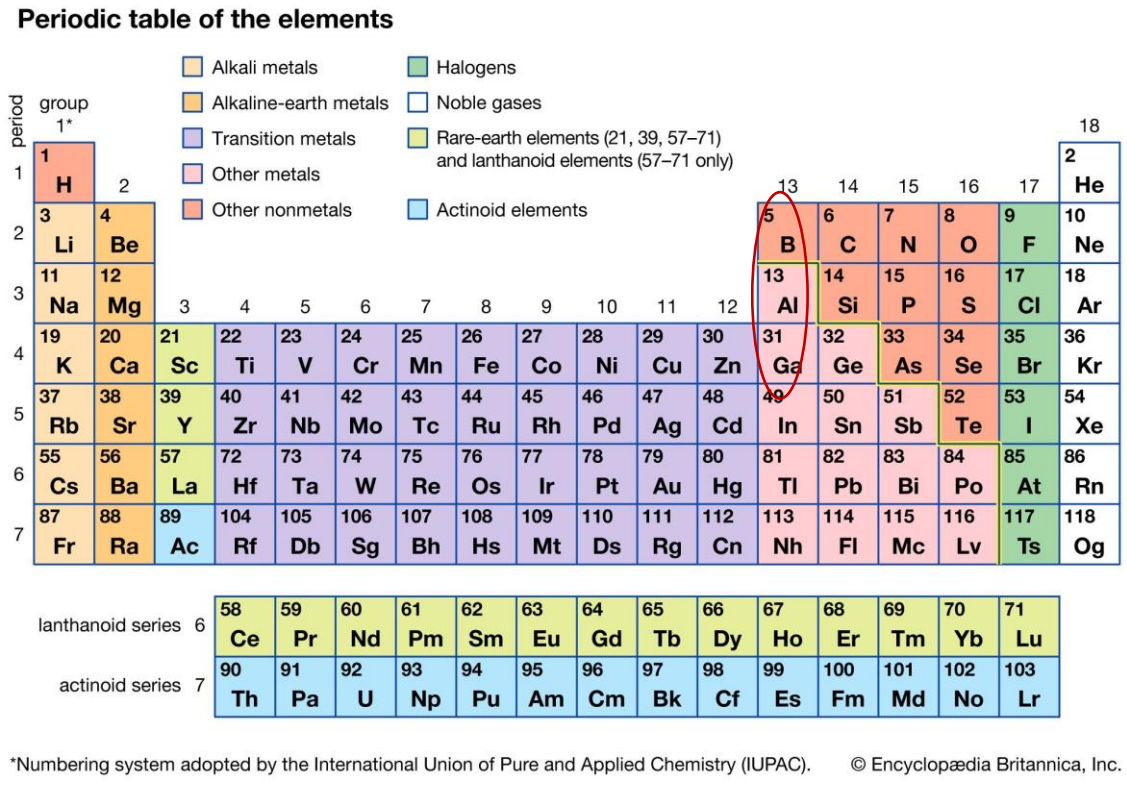

X-ray Detectors

- Only discuss electronic hard x-ray detectors.
- All use same basic principle:
  - X-ray is absorbed by atoms within detector active volume
  - Atom is ionized
  - Electrons and ions are collected by imposing high electric field across collection electrodes.
- Differences come from detector material and readout electronics.

Ionization chamber

- Photon is absorbed by gas atom
- Photoelectron and Auger electrons emitted (ionization)
- These electrons cause more ionization
- High voltage bias across plates causes electrons and ions to drift in opposite directions.
- Charges collected results in current flow which is proportional to incident x-ray intensity.

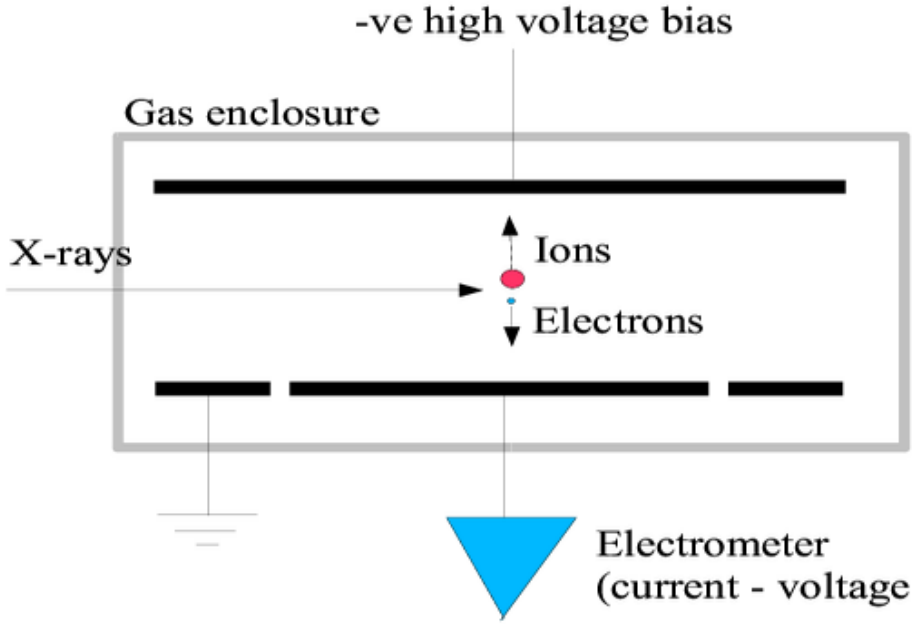

Ion Chamber: Operating voltage

- Electrons and ions like to recombine
- Bias voltage pulls them apart before they can recombine.
- Measured current increases with bias voltage until all charges are collected. This is called 'saturation'.
- Ion chambers should ALWAYS be operated in the saturation region.
- Signal currents are small: care is needed to achieve good signal / noise performance

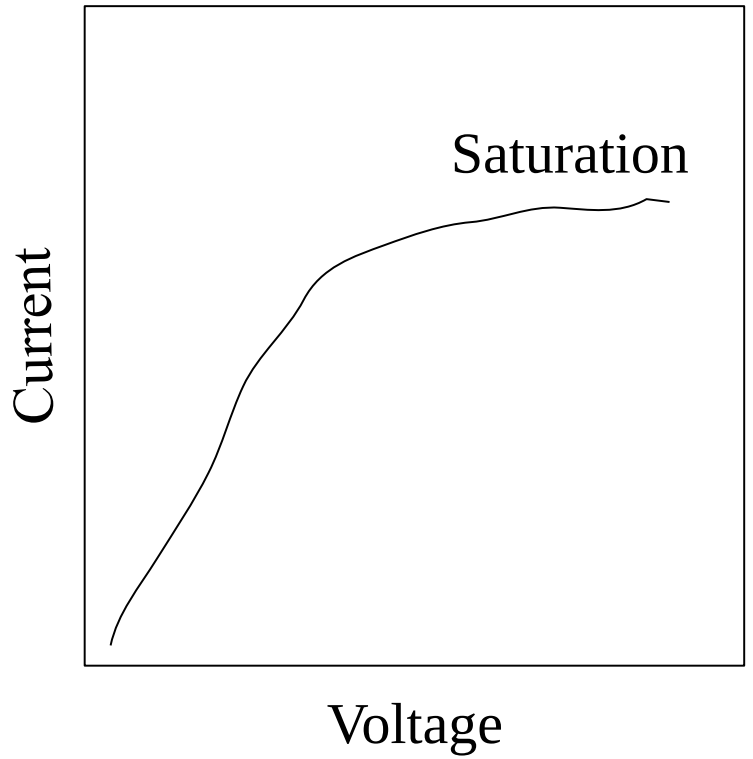

Silicon photodiodes: solid state ion chamber

- PIN or high-resistivity PN photodiodes
  - 'solid-state ion chamber'
  - modest area
  - low leakage & capacitance
  - Usually used fully depleted
- Can be used either in integrating or photon-counting mode.

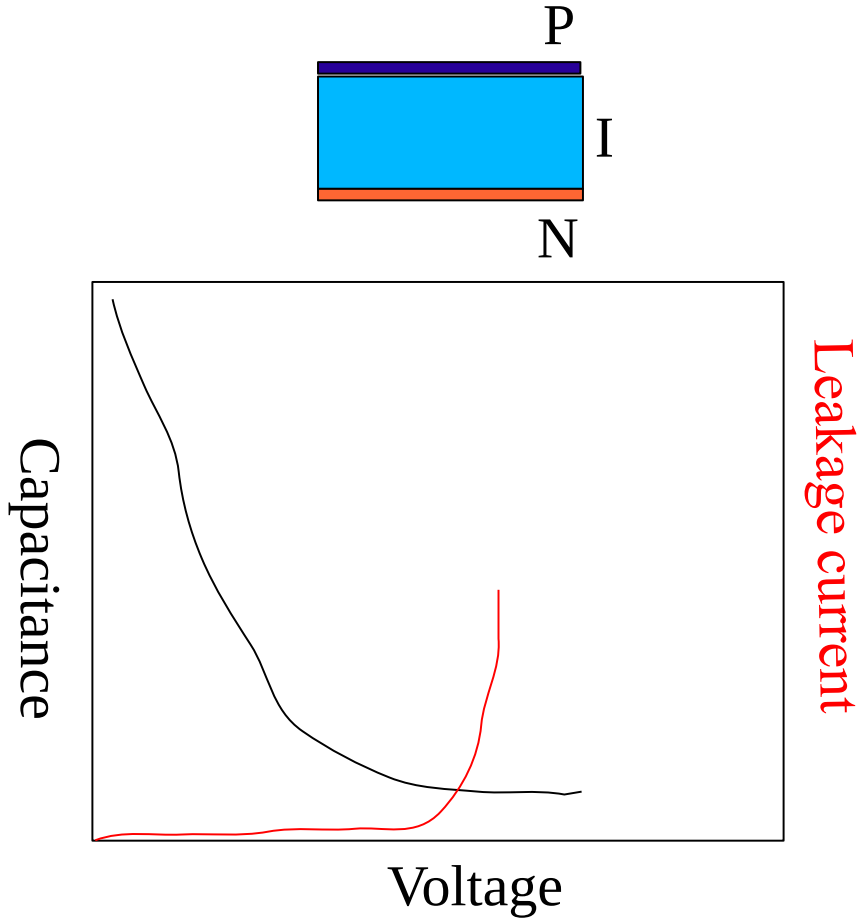

Detector types

- Integrating
  - Ionization chambers
  - Silicon diodes
    - PIN diodes
    - PN diodes on high-resistivity silicon
    - PIPS detectors
  - CCD detectors
- Photon counting
  - HPGe detector
  - Silicon diode
  - Silicon drift detector
  - Gas proportional counter
  - Avalanche photodiode

Which one to use when?

- Integrating detectors simple to operate when only interest is total intensity
  - No energy resolution

- Make use of proportionality between absorbed energy and generated charge
- Photon counting
  - Need to inspect every charge packet individually
- Amount of charge generated is small
  - $Q=E_{ph}/w * 1.6e-19$
  - w=3.6eV for silicon
  - One 8 keV photon generates 2200 electron-hole pairs in silicon
- Statistical fluctuations in number of charges determines ultimate resolution
  - Distribution is non-Poissonian: Fano factor

Detector performance Metrics

What is an ideal detector?

- ❑10^9 pixels
- ❑1μm spatial resolution
- ❑1 eV energy resolution
- ❑1 fs time resolution
- ❑Count rates up to 10^9/pixels
- ❑Efficient from few eV to 100 KeV

Detector performance Metrics

What is an ideal detector?

- ❑10^9 pixels
- ❑1μm spatial resolution
- ❑1 eV energy resolution
- ❑1 fs time resolution
- ❑Count rates up to 10^9/pixels
- ❑Efficient from few eV to 100 KeV

Brookhaven National Laboratory

Detector performance Metrics: Spatial Resolution

Ideally electrons and holes simply follow the field lines and end up on a certain electrode. So spatial resolution s the pixel pitch

Thermal diffusion drifts the charge with a rms width $\sigma_y = \sqrt{2Dt}$

Diffusion constant is related to mobility by Einstein relations $D = \frac{k_B T}{e}\mu$

Using the average field approximation $\bar{E} = V/d$ and drift velocity $v_d = \mu\bar{E}$

$$\sigma_y = \sqrt{2\frac{k_b T}{e}\frac{d^2}{V}}$$

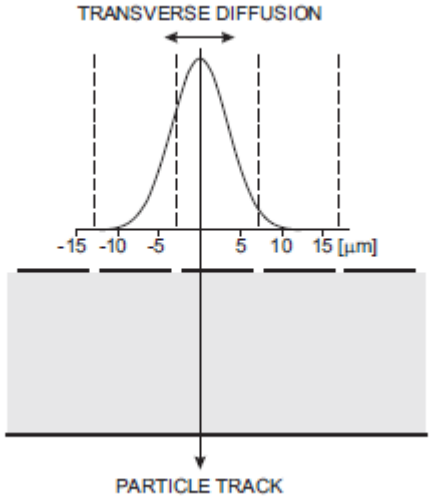

For a sensor 300 µm thick, T= 300K and V= 100V, transverse diffusion is about 7µm

Spread of charge not a bad thing! Sub-pixel resolution possible by interpolation

Detector performance Metrics: Energy Resolution

Mean ionization energy exceeds band gap because conservation of momentum requires excitation of lattice vibration.
Radiation interactions in semiconductor produces two things: Ionization and formation of electric charge pairs and lattice excitation (phonon production)

Assume that in the course of energy deposition

N_x excitations produce N_P phonons and

N_i ionization interactions form N_Q charge pairs.

On the average, the sum of the energies going into excitation and ionization is equal to the energy deposited by the incident radiation

$$E_0 = E_i N_i + E_x N_x$$

Assuming Gaussian statistics the variance in number of excitation/ionizations: $\sigma_x = \sqrt{N_x}$ and $\sigma_i = \sqrt{N_i}$
Now for a single event (single pulse) the deposited energy is constant. Hence a fluctuation in excitation must be balanced by an equivalent fluctuation in Ionization.

$$E_x \Delta N_x + E_i \Delta N_i = 0$$

If for an event more energy goes to charge formation means less energy for excitation. Averaging over several events this implies that the variance in energy for the two process must be equal:

$$E_i \sigma_i = E_x \sigma_x$$

$$\sigma_i = \frac{E_x}{E_i} \sqrt{N_x}$$

Detector performance Metrics: Energy Resolution

From the total energy $E_i N_i + E_x N_x = E_0$

$$N_x = \frac{E_0 - E_i N_i}{E_x}$$

yielding

$$\sigma_i = \frac{E_x}{E_i}\sqrt{\frac{E_0}{E_x} - \frac{E_i}{E_x} N_i}$$

Since each ionization leads to charge pair that is part of the signal

$$N_i = N_Q = \frac{E_0}{E} \quad \Rightarrow \quad \sigma_i = \sqrt{\frac{E_0}{E}} \cdot \sqrt{\frac{E_x}{E_i}\left(\frac{E}{E_i} - 1\right)}$$

Since σ_i is the variance in signal charge Q and the number of charge pairs is $N_Q = E_0/E$

$$\sigma_Q = \sqrt{F N_Q}$$

In Silicon $E_x = 0.037$ eV
$E_i = E_g = 1.1$ eV
$E = 3.6$ eV

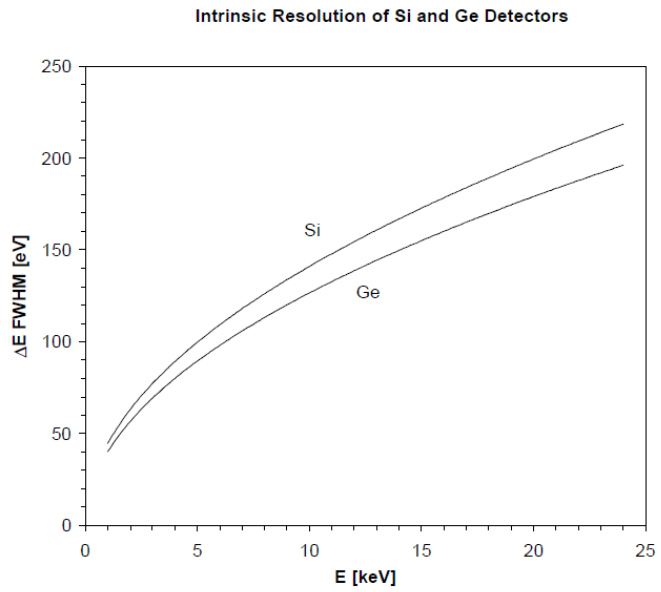

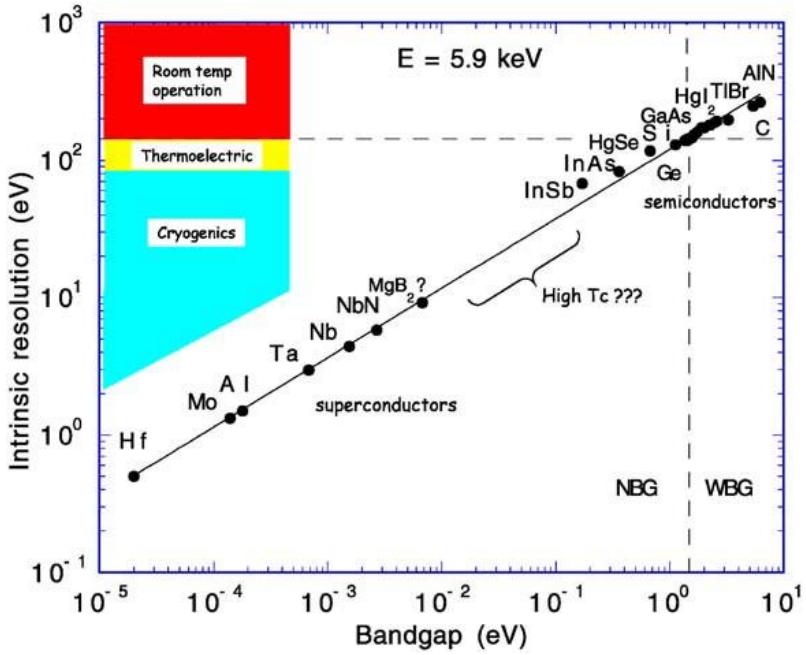

U Fano Phys Rev 72, 26 (1947)

A. Owens and A. Peacock, Nucl. Inst. Meth. Phys. Res. A., 531, 18, 2004

Brookhaven National Laboratory

Si Vs Ge

In the following we compare material properties of silicon and germanium, and discuss how these material properties affect the electrical and optical performance

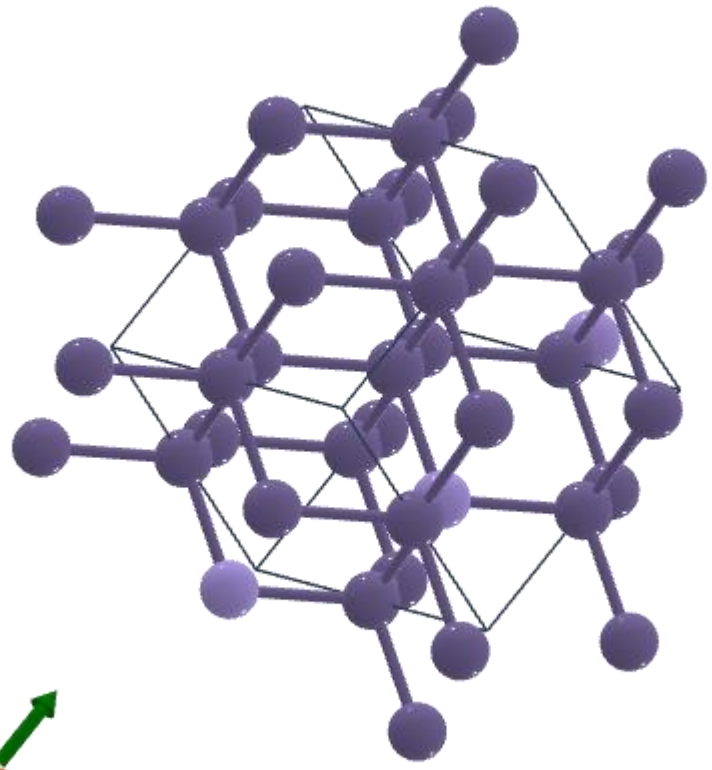

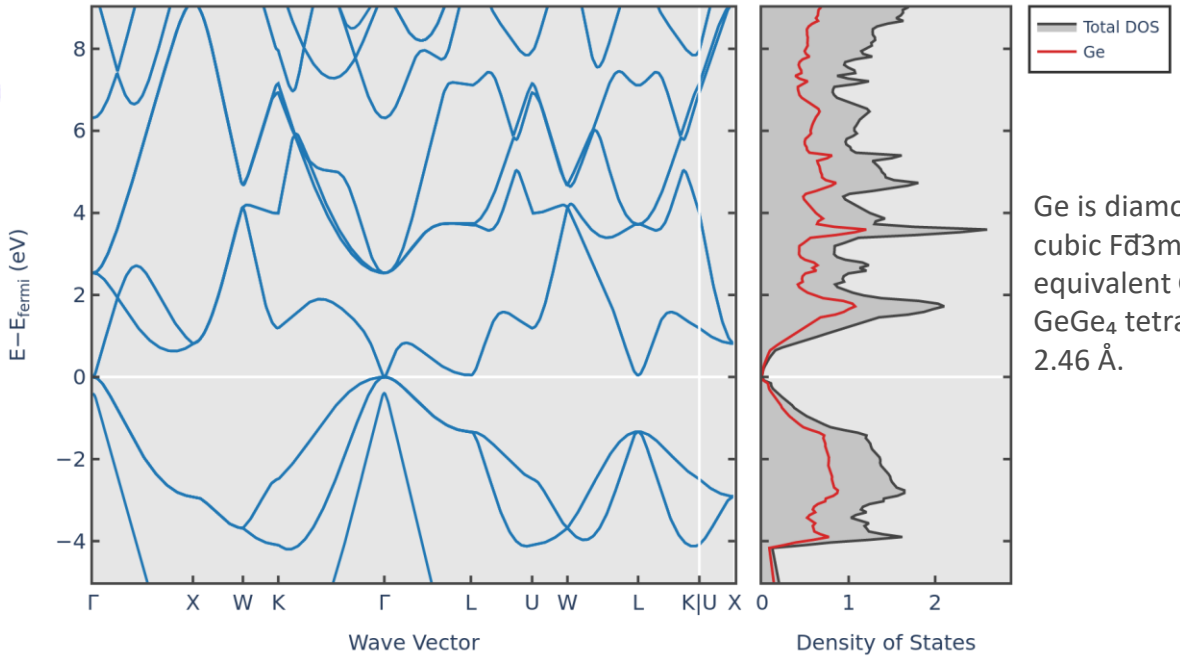

Ge is diamond structured and crystallizes in the cubic Fd̄3m space group. Ge is bonded to four equivalent Ge atoms to form corner-sharing $GeGe_4$ tetrahedra. All Ge–Ge bond lengths are 2.46 Å.

The Materials Project: https://next-gen.materialsproject.org/

Properties of Si, Ge, and GaAs

Table 1. Comparison of some basic properties of Si, Ge, and GaAs at 300 K.

Properties	Si	Ge	GaAs
Atoms/cm^3	5.02×10^{22}	4.42×10^{22}	4.42×10^{22}
Atomic weight	28.09	72.6	144.63
Breakdown field (V/cm)	$\sim 3 \times 10^5$	$\sim 1 \times 10^5$	$\sim 4 \times 10^5$
Crystal structure	Diamond	Diamond	Zincblende
Density (g/cm^3)	2.329	5.326	5.317
Dielectric constant	11.9	16.0	13.1
Effective density of states in conduction band, N_c (cm^{-3})	2.86×10^{19}	1.04×10^{19}	4.7×10^{17}
Effective density of states in valance band, N_v (cm^{-3})	1.04×10^{19}	6.0×10^{18}	7.0×10^{18}
Optical phonon energy (eV)	0.063	0.037	0.035
Effective mass (conductivity)			
Electrons (m_n/m_o)	0.26	0.082	0.067
Holes (m_p/m_o)	0.69	0.28	0.57
Electron affinity, χ (V)	4.05	4.0	4.07
Energy gap (eV)	1.12	0.67	1.42
Intrinsic carrier concentration (cm^{-3})	1.45×10^{10}	2.4×10^{13}	1.8×10^6
Intrinsic resistivity (Ω-cm)	2.3×10^5	47	10^8
Lattice constant (Å)	5.431	5.646	5.653
Melting point (°C)	1415	937	1240
Minority carrier lifetime (s)	2.5×10^{-3}	10^{-3}	$\sim 10^{-8}$
Mobility (cm^2/V·s)			
Electron (μ_n)	1,500	3900	8,500
Holes (μ_p)	450	1900	450
Thermal diffusivity (cm^2/s)	0.9	0.36	0.24
Thermal conductivity (W/cm-°C)	1.5	0.6	0.46

Courtesy: S. Holland, LBNL

Table 1. Comparison of some basic properties of Si, Ge, and GaAs at 300 K.			
Properties	Si	Ge	GaAs
Atoms/cm^3	5.02×10^{22}	4.42×10^{22}	4.42×10^{22}
Atomic weight	28.09	72.6	144.63
Breakdown field (V/cm)	$\sim 3 \times 10^5$	$\sim 1 \times 10^5$	$\sim 4 \times 10^5$

Table 1. Comparison of some basic properties of Si, Ge, and GaAs at 300 K.		
Properties	Si	Ge
Energy gap (eV)	1.12	0.67

Effective mass (conductivity)			
Electrons (m_n/m_o)		82	0.067
Holes (m_p/m_o)		28	0.57
Electron affinity, χ (V)		0	4.07
Energy gap (eV)		67	1.42
Intrinsic carrier concentration (cm^{-3})		10^{13}	1.8×10^6
Intrinsic resistivity (Ω-cm)		7	10^8
Lattice constant (Å)		46	5.653
Melting point (°C)	1415	937	1240
Minority carrier lifetime (s)	2.5×10^{-3}	10^{-3}	$\sim 10^{-8}$
Mobility (cm^2/V·s)			
Electron (μ_n)	1,500	3900	8,500
Holes (μ_p)	450	1900	450
Thermal diffusivity (cm^2/s)	0.9	0.36	0.24
Thermal conductivity (W/cm-°C)	1.5	0.6	0.46

$$\lambda_{cutoff} \approx \frac{1.24}{E_g}$$

Courtesy: S. Holland, LBNL

Si Vs Ge

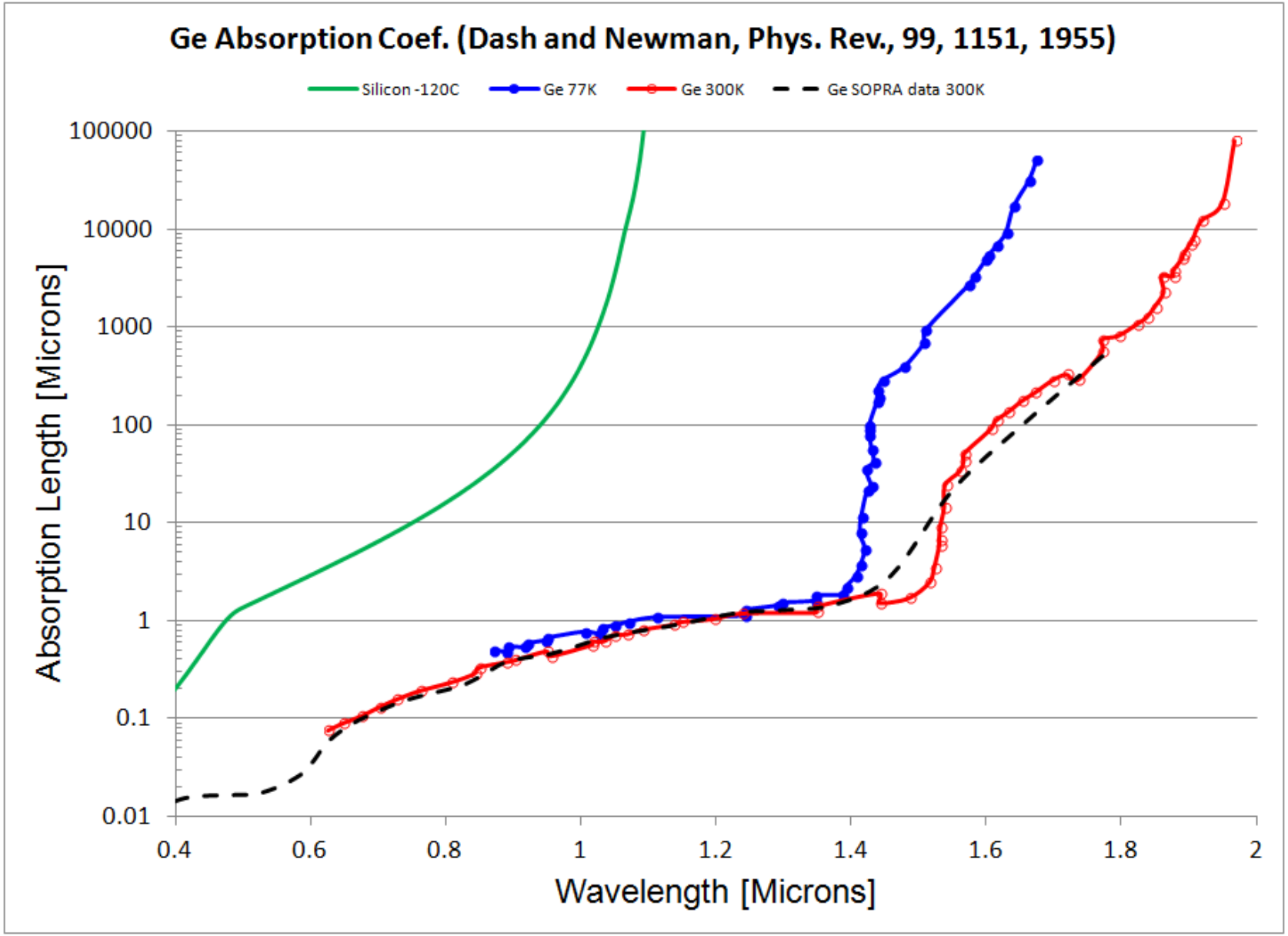

Brookhaven National Laboratory

Table 1. Comparison of some basic properties of Si, Ge, and GaAs at 300 K.

Properties	Si	Ge	GaAs
Atoms/cm^3	5.02×10^{22}	4.42×10^{22}	4.42×10^{22}
Atomic weight	28.09	72.6	144.63
Breakdown field (V/cm)	$\sim 3 \times 10^5$	$\sim 1 \times 10^5$	$\sim 4 \times 10^5$

Table 1. Comparison of some basic properties of Si, Ge, and GaAs at 300 K.

Properties	Si	Ge
Atomic weight	Z = 14 28.09	Z = 32 72.6
Density (g/cm^3)	2.329	5.326

Holes (m_p/m_o)	0.69	0.28	0.57
Electro			
Energy			
Intrinsi			
Intrinsi			
Lattice			
Melting			
Minorit			
Mobility (cm^2/V·s)			
Electron (μ_n)	1,500	3900	8,500
Holes (μ_p)	450	1900	450
Thermal diffusivity (cm^2/s)	0.9	0.36	0.24
Thermal conductivity (W/cm-°C)	1.5	0.6	0.46

Ge is 2.3x denser than silicon
Good for γ and x-ray detection
Practical issue: wafers are heavy

Courtesy: S. Holland, LBNL

Si Vs Ge

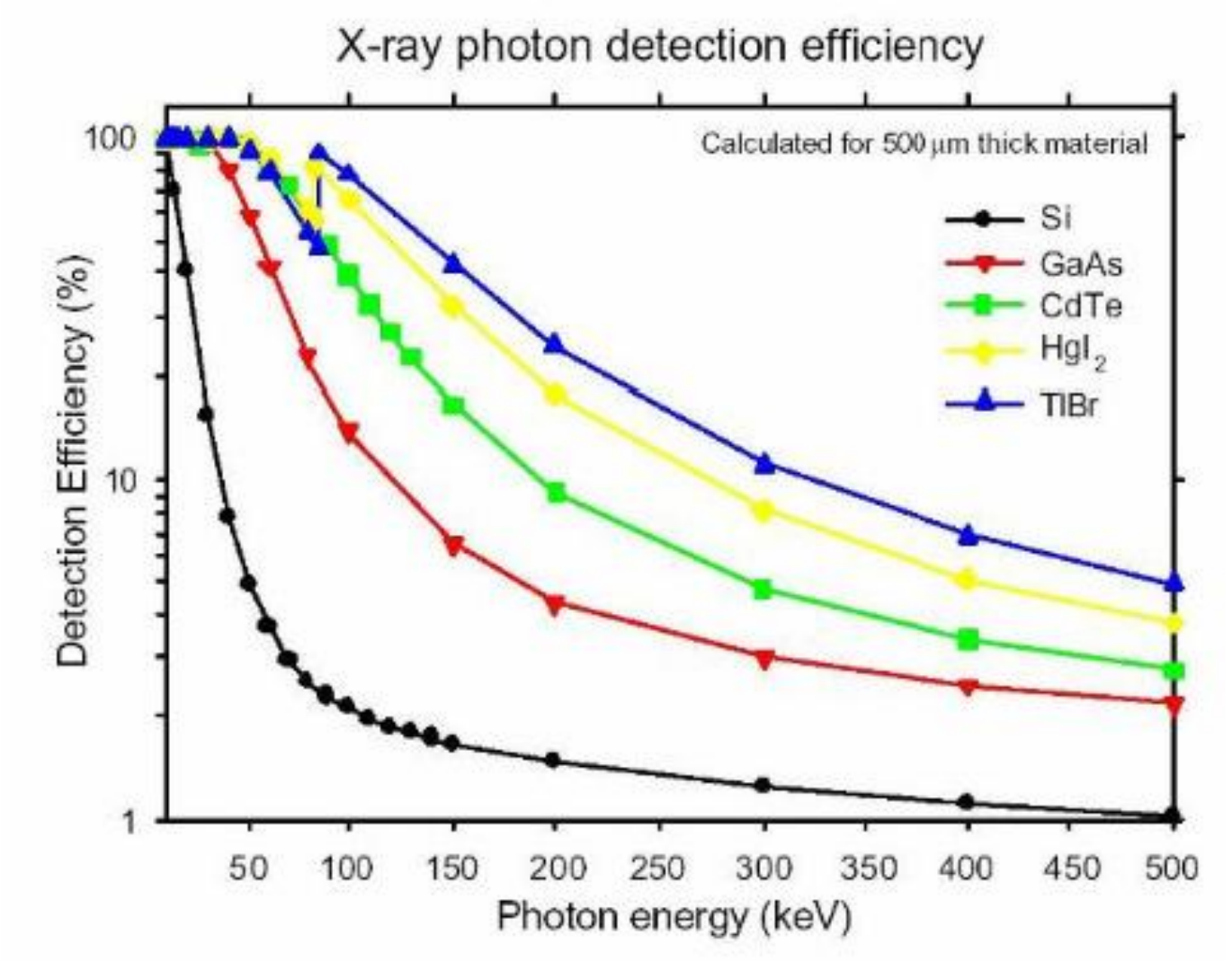

Brookhaven National Laboratory

Table 1. Comparison of some basic properties of Si, Ge, and GaAs at 300 K.

Properties	Si	Ge	GaAs
Atoms/cm^3	5.02×10^{22}	4.42×10^{22}	4.42×10^{22}
Atomic weight	28.09	72.6	144.63
Breakdown field (V/cm)	$\sim 3 \times 10^5$	$\sim 1 \times 10^5$	$\sim 4 \times 10^5$

Table 1. Comparison of some basic properties of Si, Ge, and GaAs at 300 K.

Properties	Si	Ge
Energy gap (eV)	1.12	0.67
Intrinsic carrier concentration (cm^{-3})	1.45×10^{10}	2.4×10^{13}
Minority carrier lifetime (s)	2.5×10^{-3}	10^{-3}

Holes (m_p/m_o) 0.69 0.28 0.57

Electro

Energy

Intrinsi

Intrinsi

Lattice

Melting

Minorit

$$J_{leakage} \propto \frac{n_i}{\tau_g} \propto \frac{\exp(-E_g/2kT)}{\tau_g}$$

Mobility (cm^2/V·s)			
Electron (μ_n)	1,500	3900	8,500
Holes (μ_p)	450	1900	450
Thermal diffusivity (cm^2/s)	0.9	0.36	0.24
Thermal conductivity (W/cm-°C)	1.5	0.6	0.46

Courtesy: S. Holland, LBNL

Si Vs Ge

Ideal dark current for Si Vs Ge, assumption Si forced to ~ 1 nA/Sq, and same τ_g

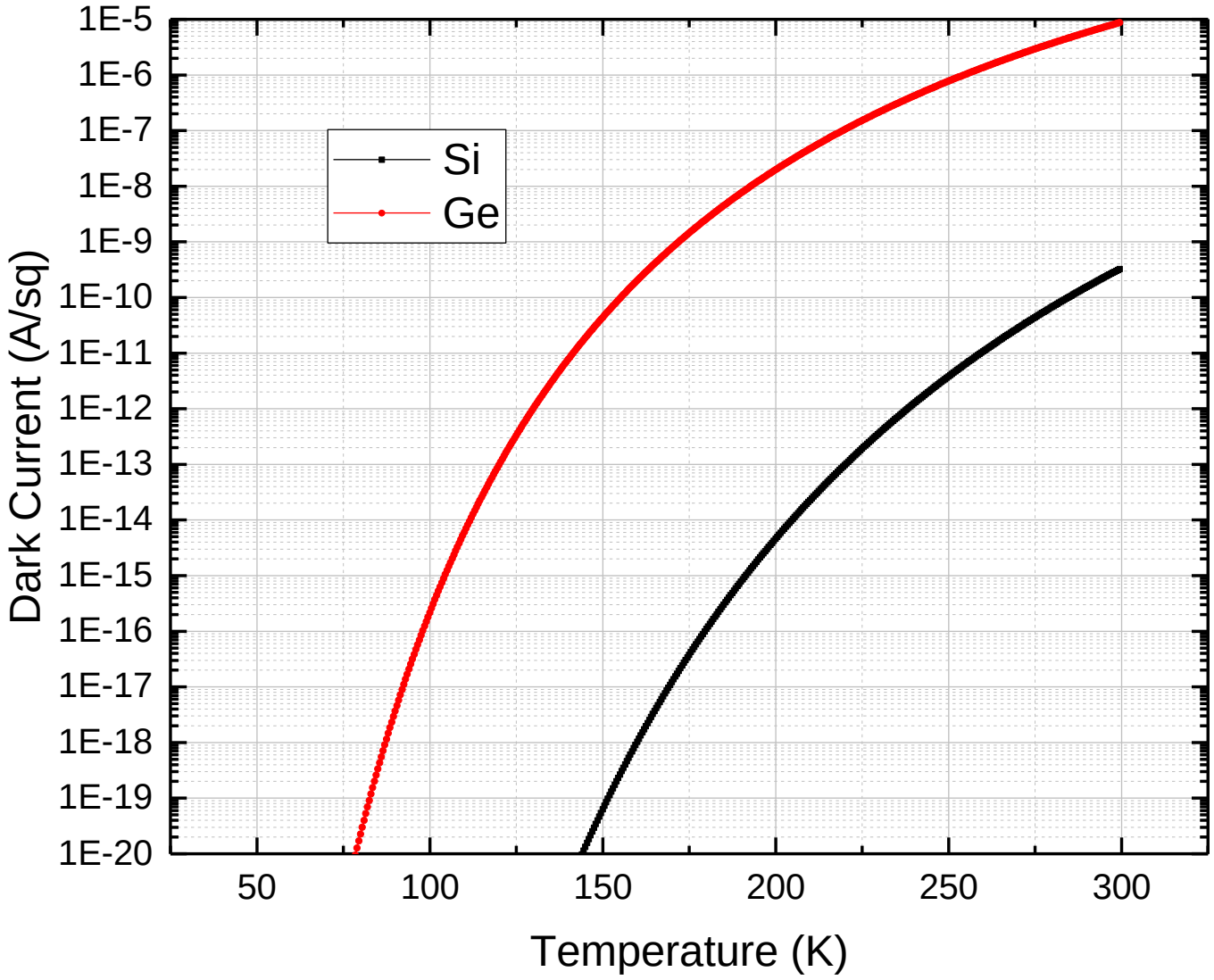

Needs Cryo-cooling !

Brookhaven National Laboratory

Germanium: First transistor

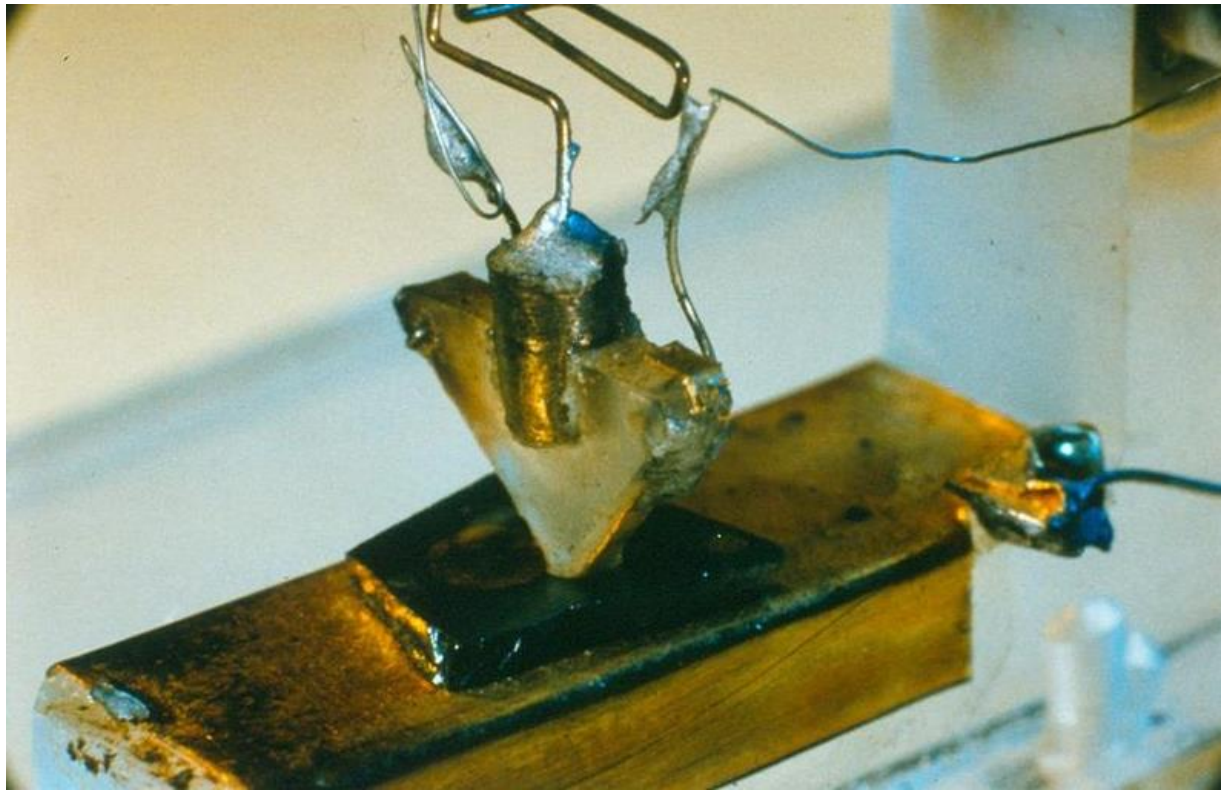

First Transistor: Bardeen, Brattain, and Shockley, Bell Labs, 1947

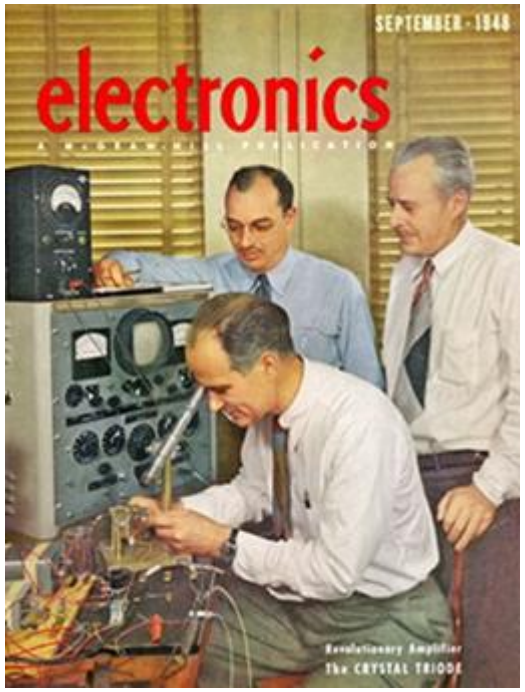

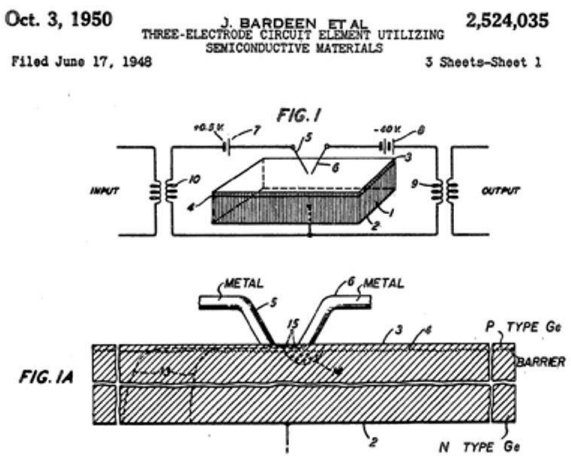

- Germanium was easy to purify because of lower melting point
- Not until 1954, Texas Instruments demonstrated the silicon grown junction transistor

Brief history of transistor

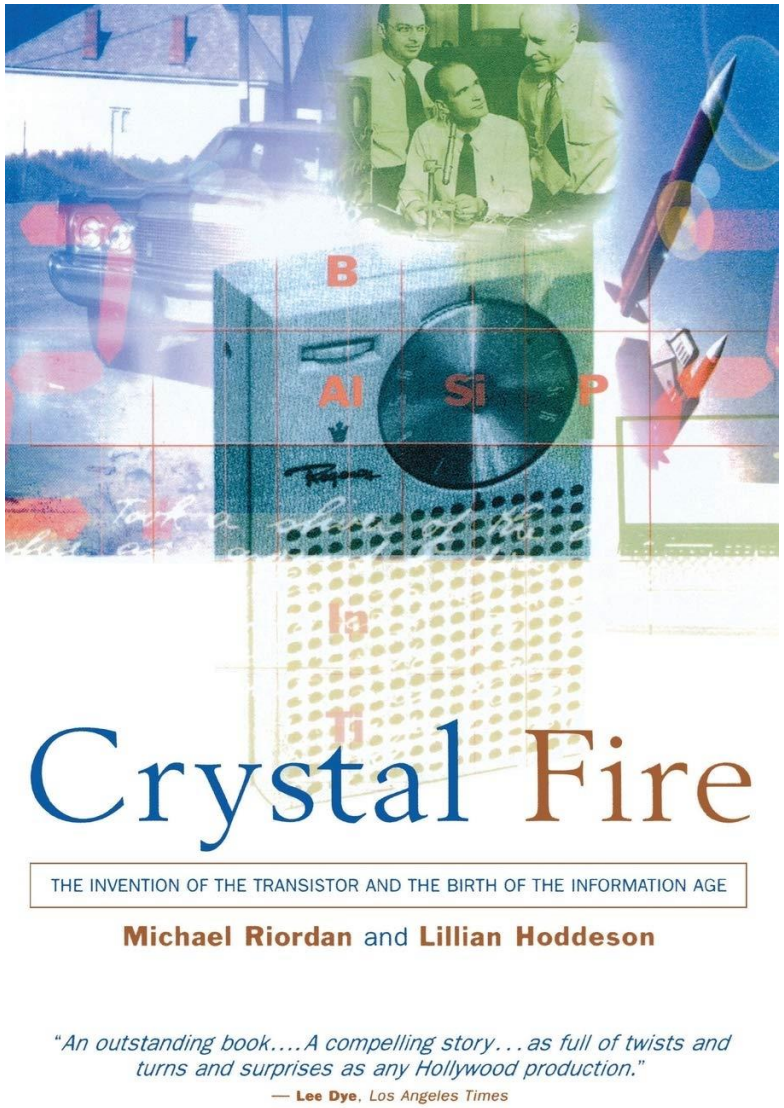

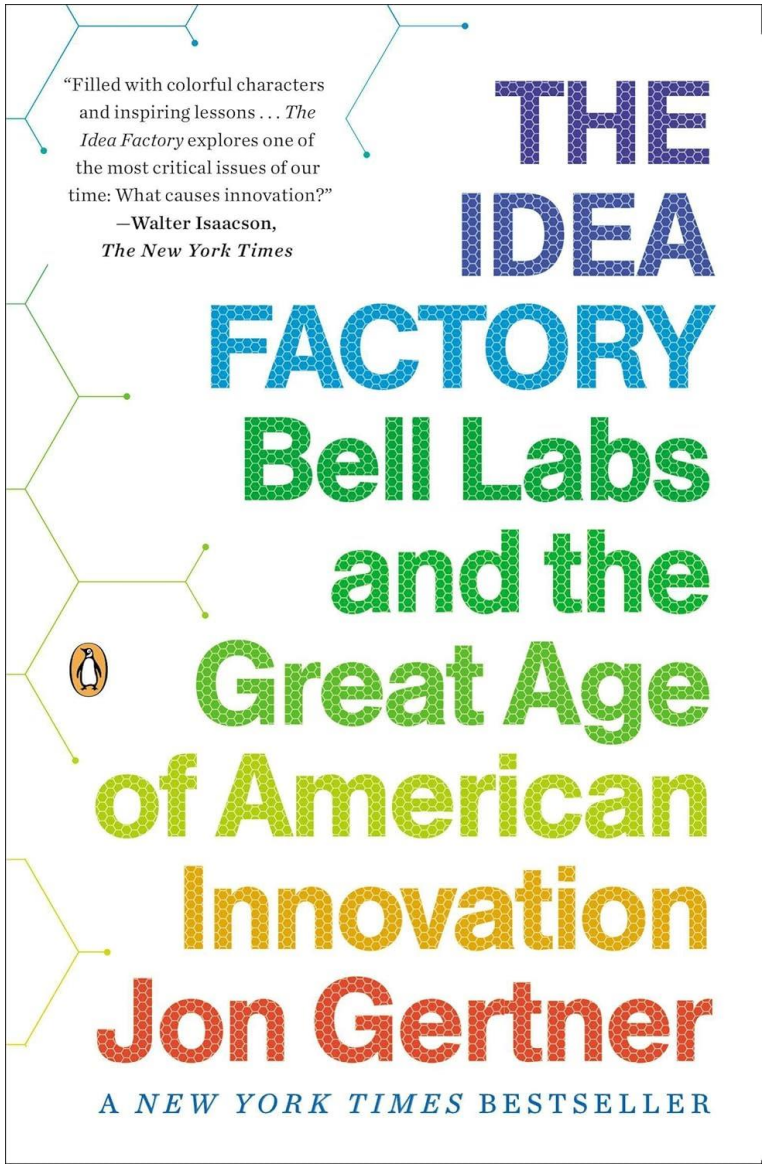

Brookhaven National Laboratory

Si Vs Ge

Table 1. Comparison of some basic properties of Si, Ge, and GaAs at 300 K.

Properties	Si	Ge
Mobility ($cm^2/V \cdot s$)		
Electron (μ_n)	1,500	3900
Holes (μ_p)	450	1900

- Germanium has high carrier mobilities
- Ge has the largest hole mobility of any semiconductor
- Renewed interest in Ge due to high-mobilities

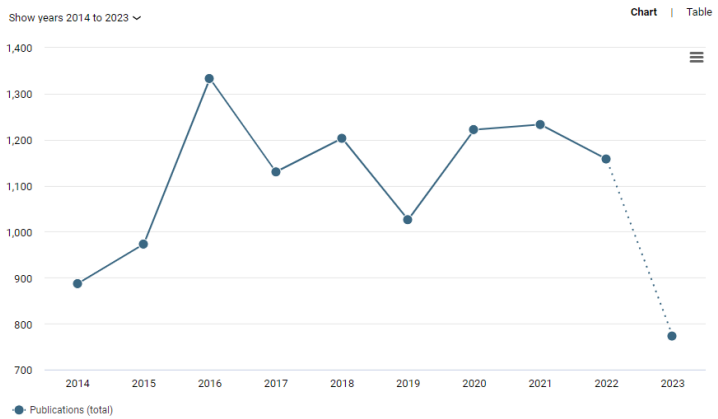

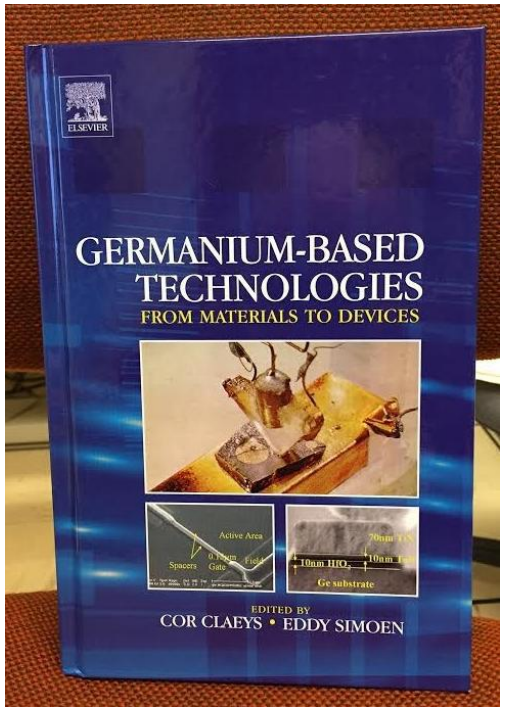

Brookhaven National Laboratory

Ge Issues

- Technology not as mature as Si
- Key to devices (and detectors) are field oxides
- GeO_2 is unstable (water soluble) and thermally unstable at temperatures normally employed for device processing.
- High-K dielectrics?
- Capping of Ge/GeO_2 with other oxides

Brattain and Bardeen first test

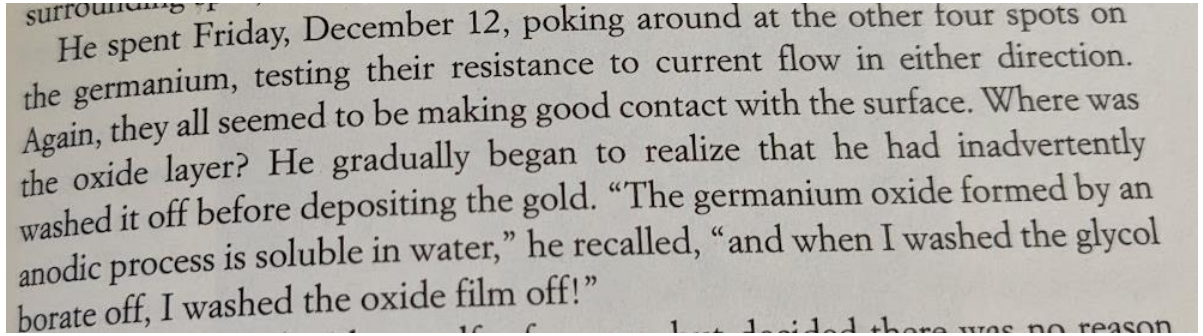

He spent Friday, December 12, poking around at the other four spots on the germanium, testing their resistance to current flow in either direction. Again, they all seemed to be making good contact with the surface. Where was the oxide layer? He gradually began to realize that he had inadvertently washed it off before depositing the gold. "The germanium oxide formed by an anodic process is soluble in water," he recalled, "and when I washed the glycol borate off, I washed the oxide film off!"

ACS APPLIED MATERIALS & INTERFACES

Research Article

www.acsami.org

Stabilization of the GeO_2/Ge Interface by Nitrogen Incorporation in a One-Step NO Thermal Oxynitridation

Gabriela Copetti,[†] Gabriel V. Soares,[†] and Cláudio Radtke*[,‡]

[†]Instituto de Física and [‡]Instituto de Química, UFRGS, 91509-900 Porto Alegre, Brazil

However, the lack of a stable passivation layer for Ge surface hinders the development of such technology. Unlike silicon dioxide (SiO_2), germanium dioxide (GeO_2) is water-soluble and also thermally unstable at temperatures usually employed during device processing.[2] This instability is due to the interfacial reaction $GeO_2 + Ge \rightarrow 2GeO$ that occurs at temperatures greater than 400 °C. Oxygen vacancies generated at the GeO_2/Ge interface diffuse through the oxide toward the surface, where they promote GeO desorption (as evidenced by thermal desorption spectroscopy[3]), leading to the deterioration of the device's electrical properties.[4] First-principles calculations predicted that

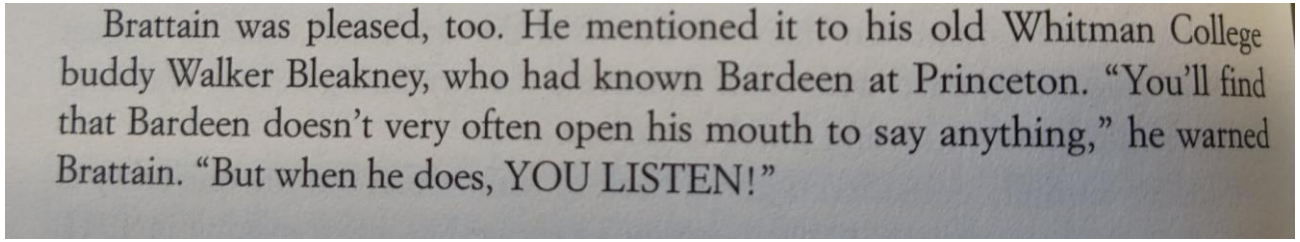

Brattain was pleased, too. He mentioned it to his old Whitman College buddy Walker Bleakney, who had known Bardeen at Princeton. "You'll find that Bardeen doesn't very often open his mouth to say anything," he warned Brattain. "But when he does, YOU LISTEN!"

Brookhaven National Laboratory

Pixel Isolation with Trenches

- Sensors for radiation detections are in micron scale (not nm!)
- Simple devices can be fabricated with few masks
- Pixels isolation with physical trenches

Isolation with trenches

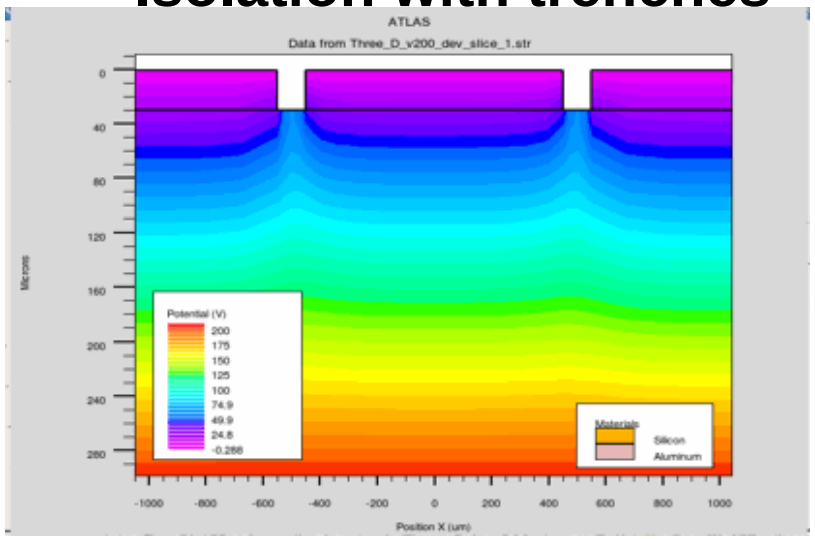

A.Hamacher et al. Nucl.Ins. Meth.Phys. Res. **A295**, 128 (1990)

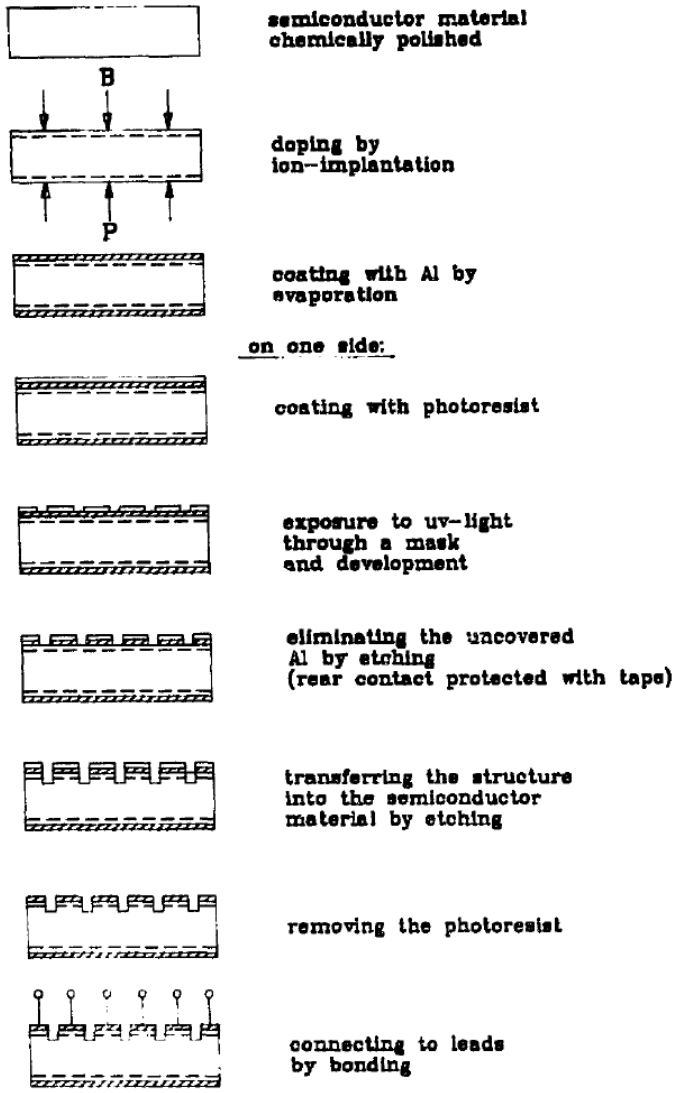

Brookhaven National Laboratory

Ge sensors with trenches

- P-type layer formed by ion implantation.
- N-type contact formed by diffusion.
- Implanted layer formed into pixels by etching trenches between them.
- Pixels become electrically isolated upon full depletion.

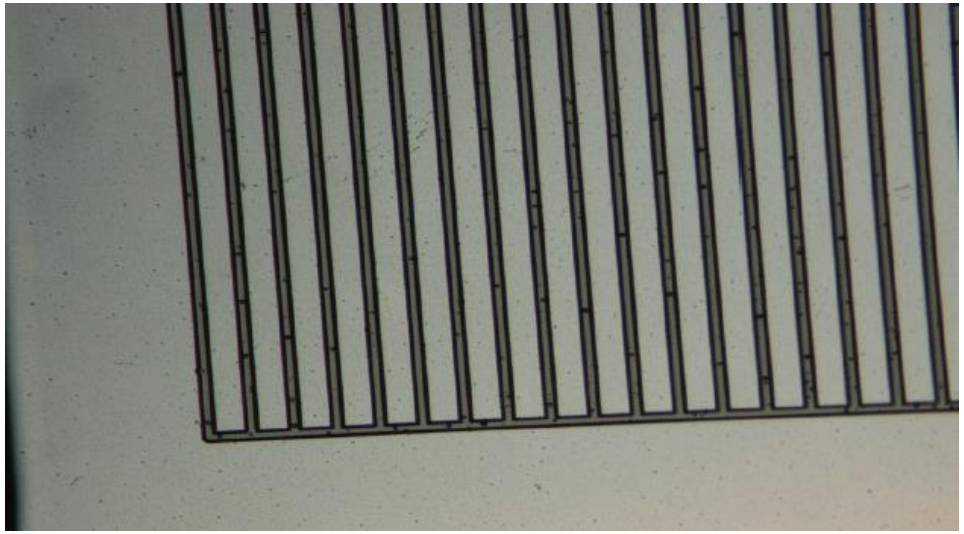

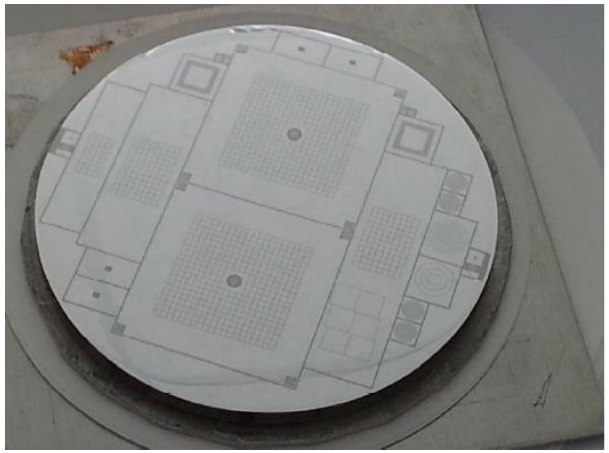

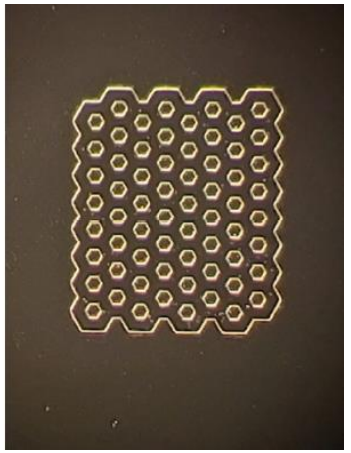

ASIC: MARS, a new spectroscopy chip

MARS has 32 low-noise channels, each with its own peak detector and timing circuitry
– Charge-sensitive preamplifier capable of reading electrons or holes, with 4 gain settings from 3600mV/fC to 600mV/fC (12.5keV – 75keV F.S.)
– Shaper with 4 time constants from 0.25 us to 2 us.
– Per-channel peak detector and timing generator. Timing generator can measure time-over-threshold (for pileup detection) or time-of-arrival (for detecting charge-shared events)
– All external signals are fully differential to preserve the system's low noise

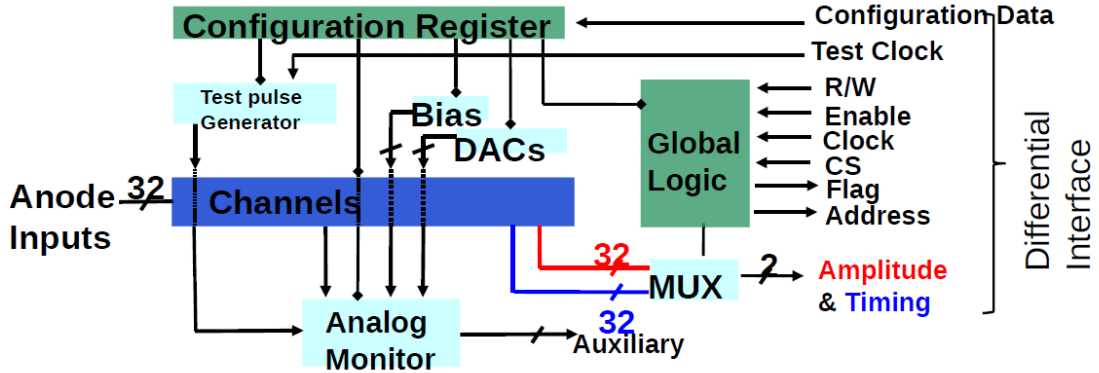

32 readout channels
• Amplitude and timing measurement per channel
• LVDS interface, analog differential outputs
• Test pulse generator
• Multiplexed analog monitors

Multi-element Germanium prototype: 64-strip

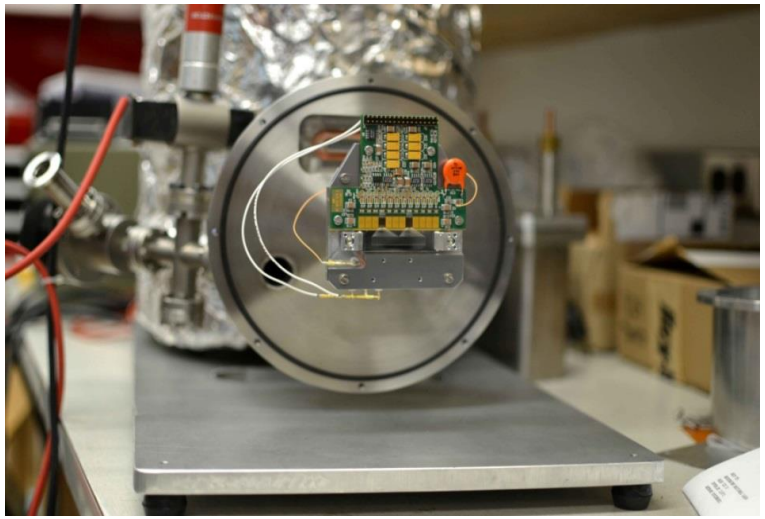

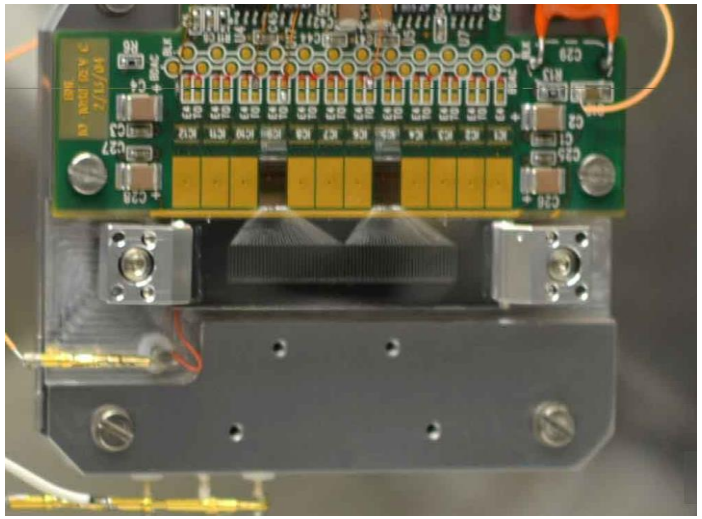

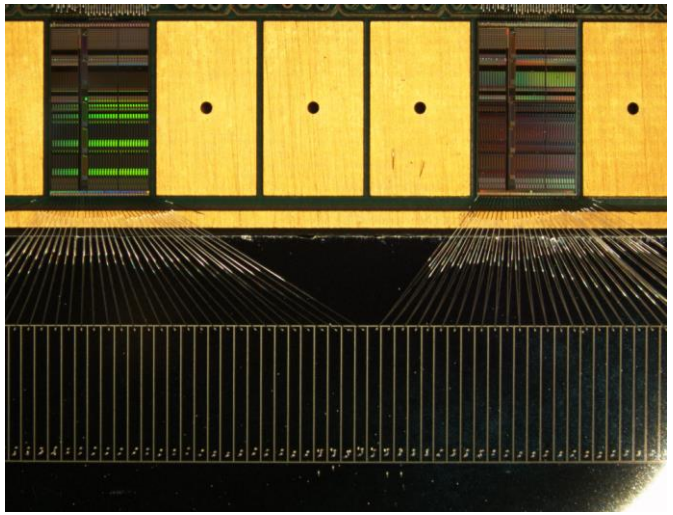

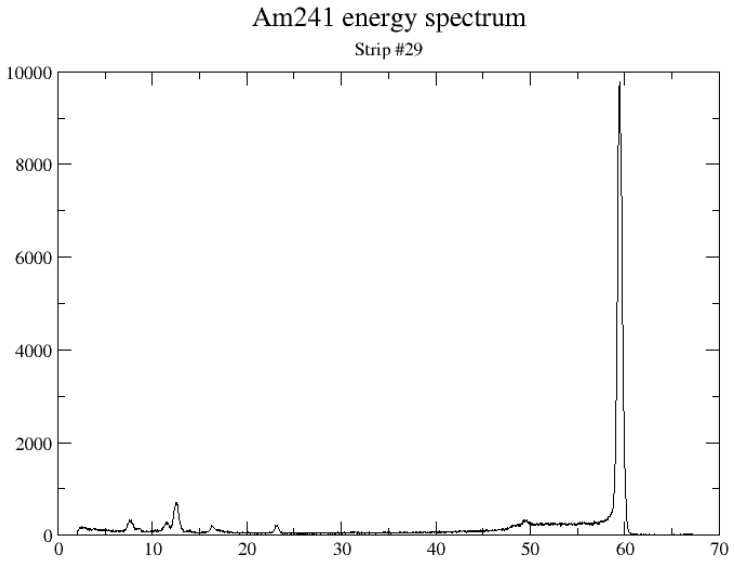

Energy resolution:
~450eV @ 60keV

Multi-element Germanium prototype: what do we do with it?

Recall: Bragg's law

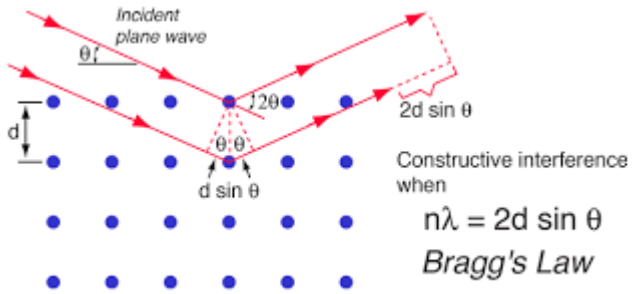

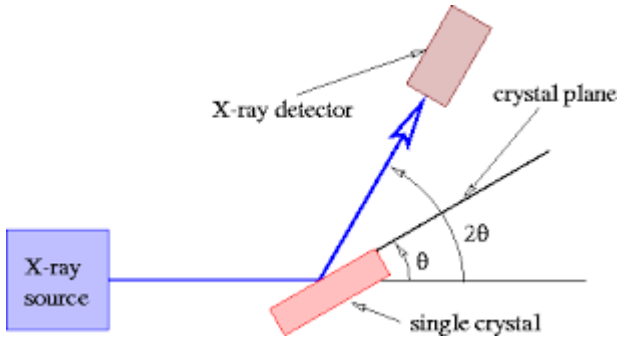

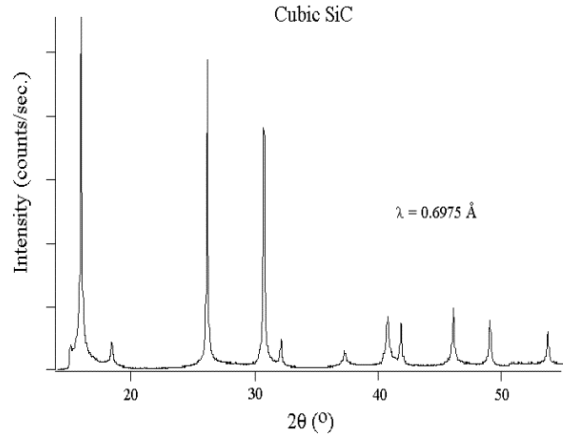

Energy Dispersive X-ray Diffraction with 64-Ge Strip Detector

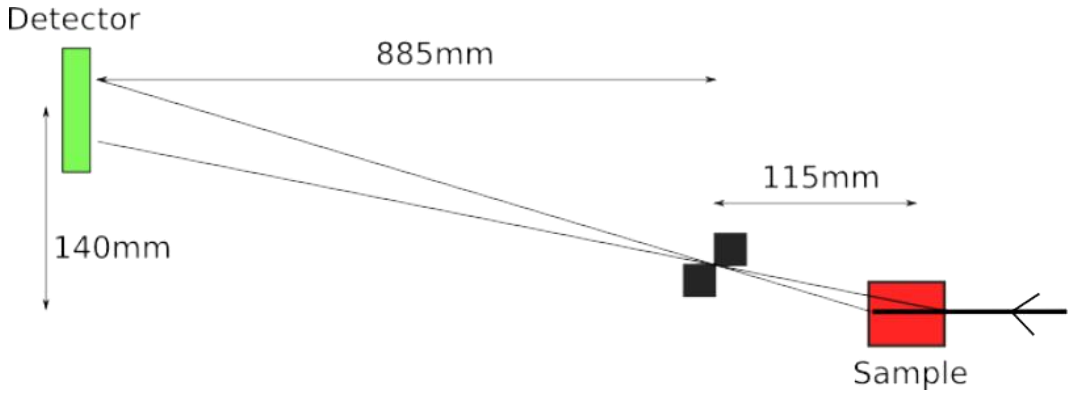

- 100um white beam enters from right
- Slit projects scattered beams onto strip detector
- Each detector element collects spectra (i.e. diffraction pattern) from one region of sample.

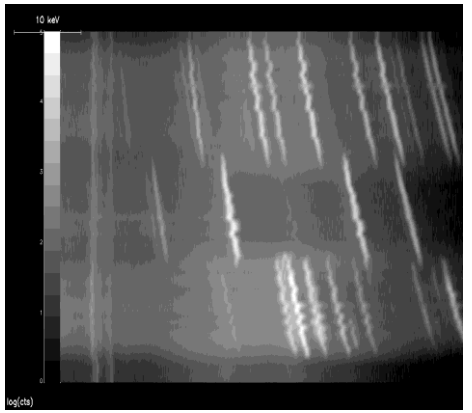

Image: http://ffden-2.phys.uaf.edu/211.fall2000.web.projects/Casey%20Hedlund/default.htm

Brookhaven National Laboratory

Multi-element Germanium prototype: what do we do with it?

Energy dispersive diffraction imaging

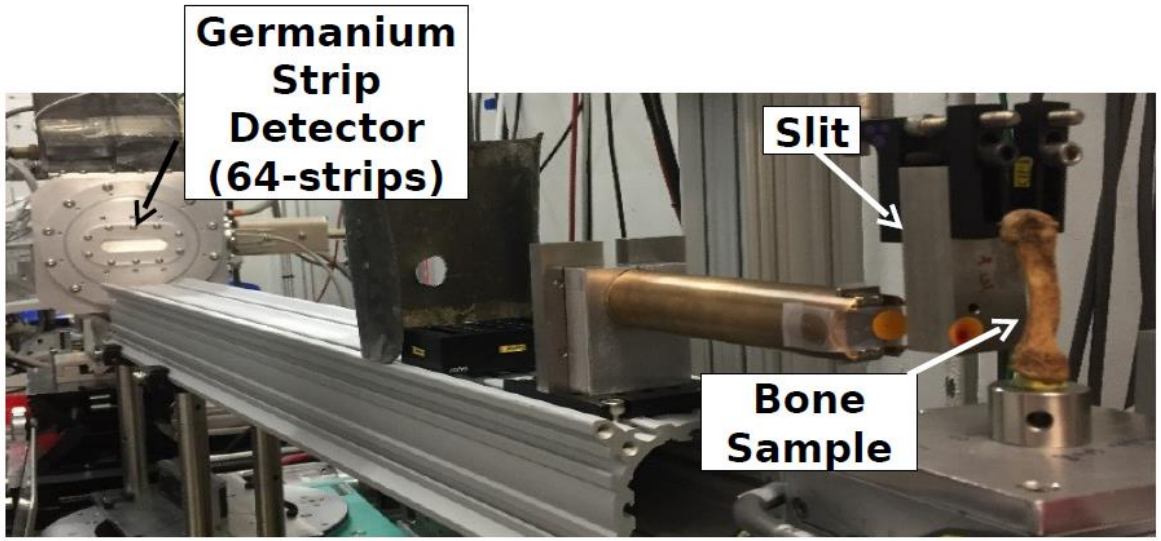

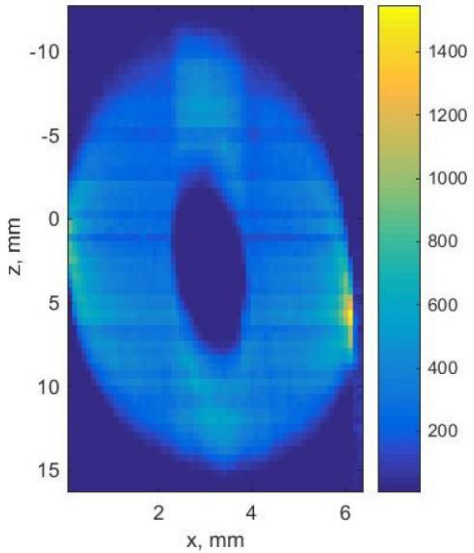

- The energy dispersive real space reconstruction of a hydroxyapatite (hAp) bone phantom is shown to the left.
- Several diffraction peaks were reconstructed and peak intensity from one is shown here (hAp 004 reflection).
- The shape including empty central region is correctly reconstructed.
- Peak centers from each phase present can also be reconstructed to yield strain information.

Brookhaven National Laboratory

S R Stock et. al, Proc SPIE 10391, 103910A (2017)
A.K. Rumaiz, T. Krings, D.P. Siddons, A.J. Kuczewski, D. Protic, C. Ross, G. De. Geronimo and Z. Zhong, IEEE Trans. Nucl. Sci., 61, 3721 (2014)

384-element detector: XPD beamline, NSLS II

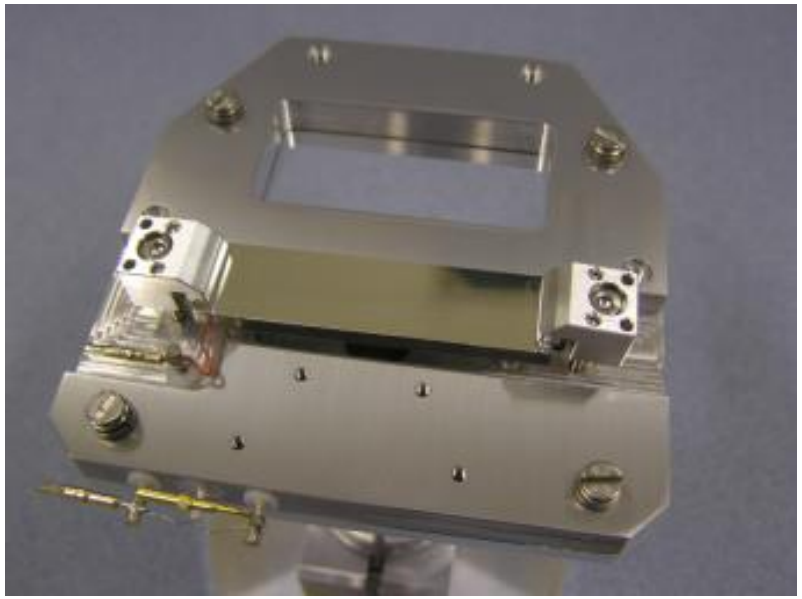

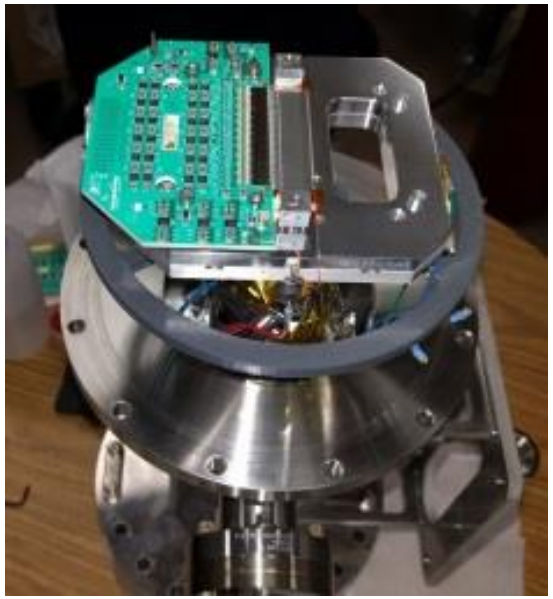

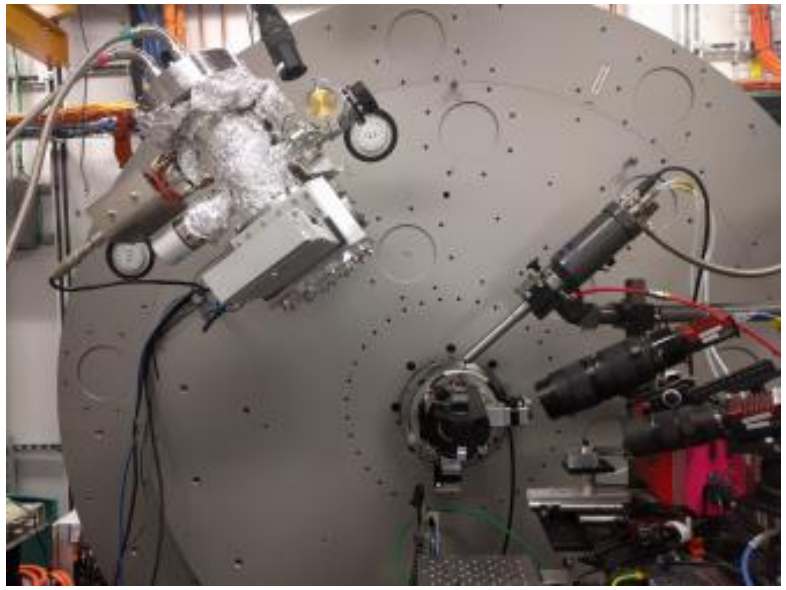

For this application we built a 384-strip detector
– 384 strips, 0.125 mm x 8mm
– 3mm thick
– 12 ASICs with full parallel readout

Time-stamping events enables dynamic measurements

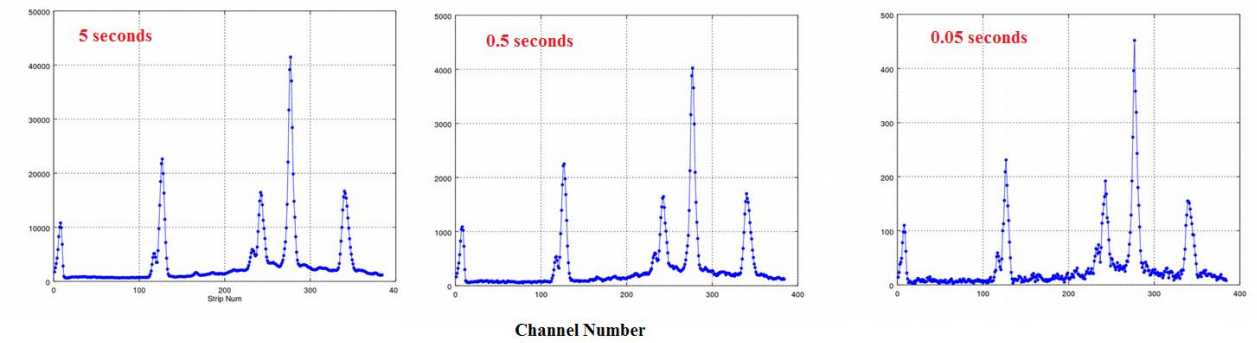

Brookhaven National Laboratory

New Germanium detectors at BNL: Present

7 Channel Ge pixel with low-noise readout

- Energy resolving Silicon drift sensor is the detector of choice for XAFS beamline. However, are very inefficient above 15 KeV
- High-purity Germanium (HPGe) on the other hand offers excellent energy resolution and detection efficiency for high-energy X-ray.
- Problem of Si escape peak being close to the absorption edge can be resolved with Ge (K_α~ 9.8 KeV).

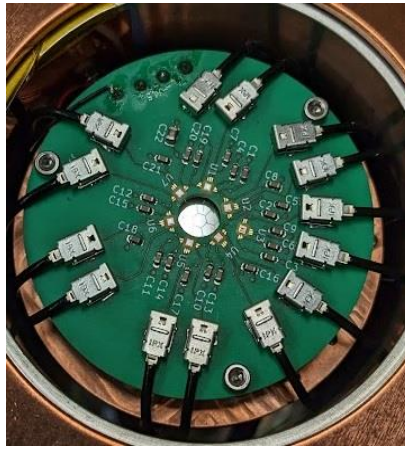

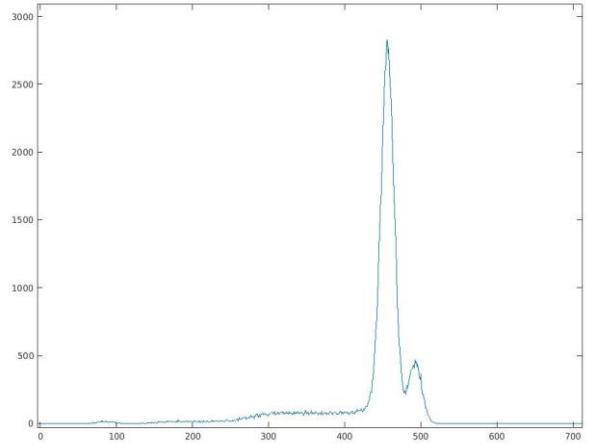

Energy resolution ~260 eV
Cube PRE_39 ~ 20 e ENC@ 1 µs

Extended X-ray Absorption Fine Structure (EXAFS)

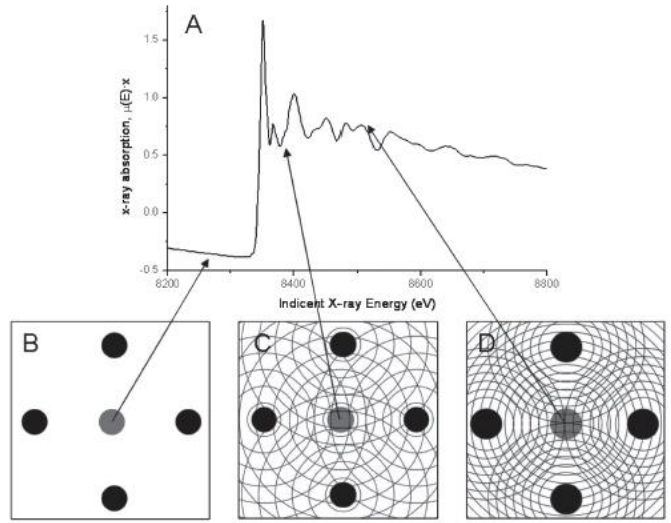

S. D. Shelly et al. in Methods of Soil Analysis: Part 5 (2008) Soil Science Society of America

Fluorescence Imaging with MAIA Detector

Traditionally done with Silicon drift array. Scan over larger area is time consuming
MAIA (384 p-i-n diodes) on the fly scanning: Faster scan time.
Detector limits the energy that can be scanned (less than 20 KeV)
Rely on *L* lines for high-Z materials

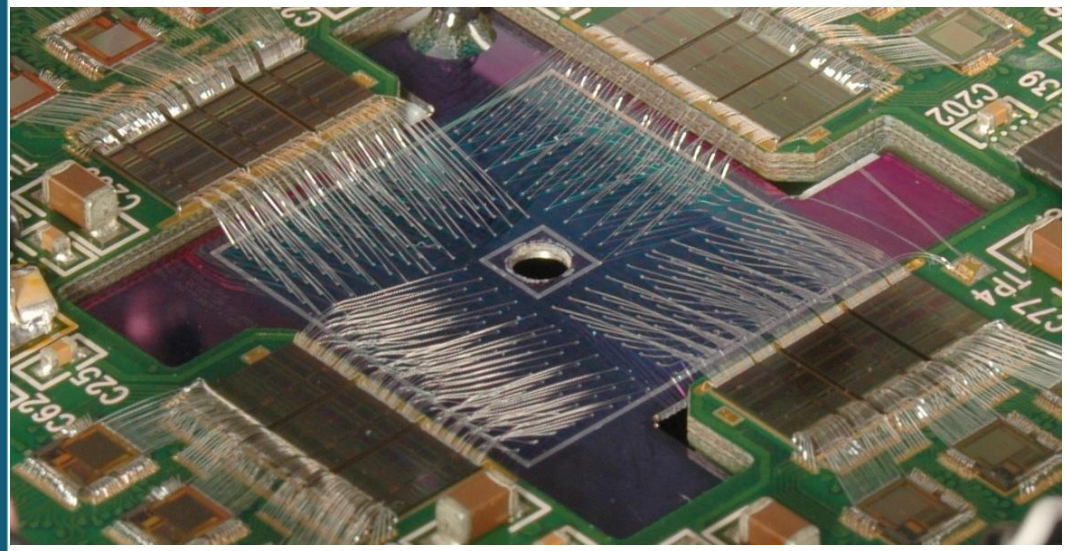

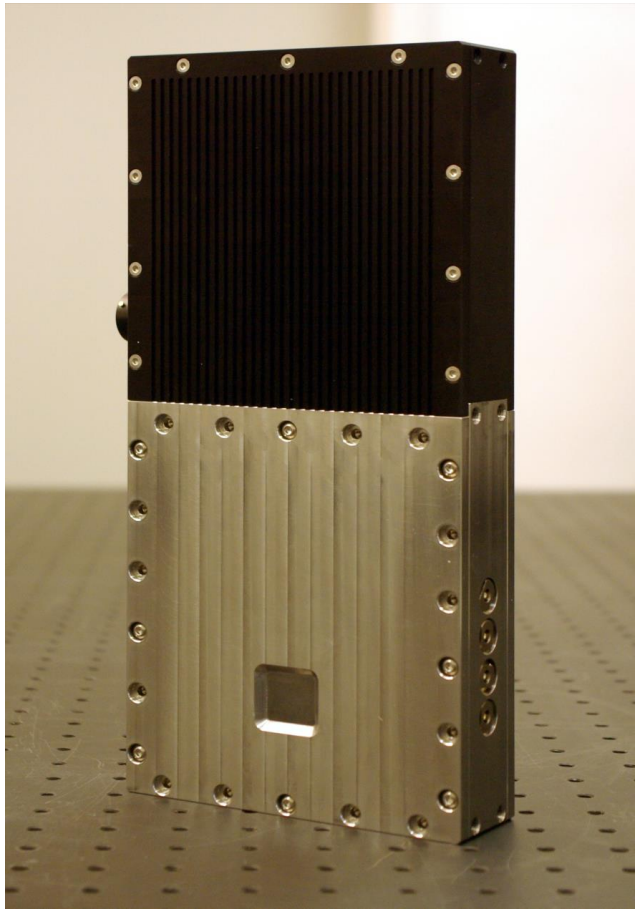

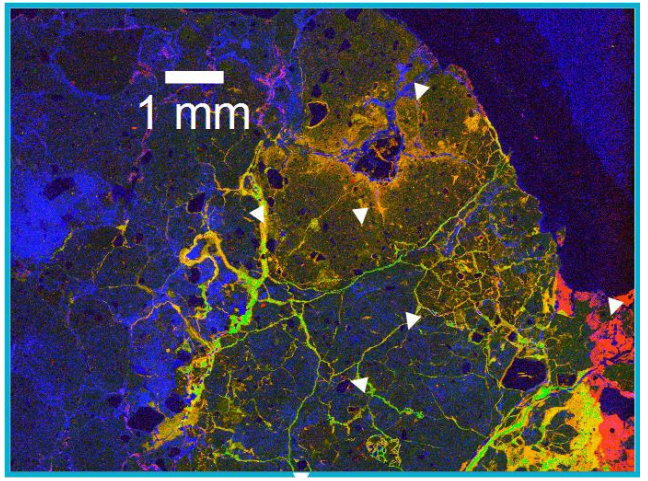

Rob Hough, James Cleverley, CSIRO, private communication

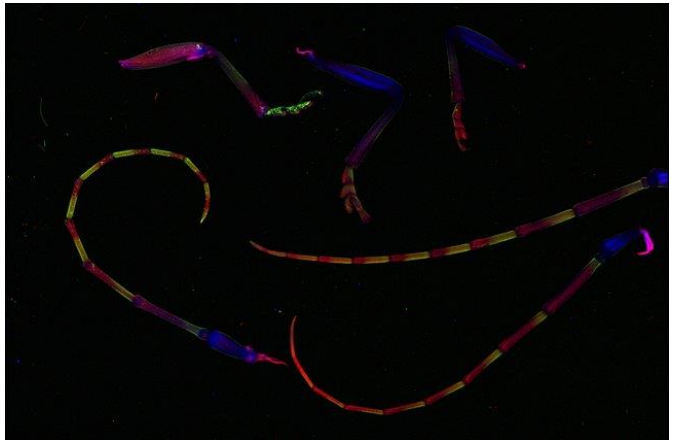

Brookhaven National Laboratory

96- pixel Germanium detector (Ge version of Maia: Gaia)

96-germanium pixel sensor wire bonded to HE-MARS

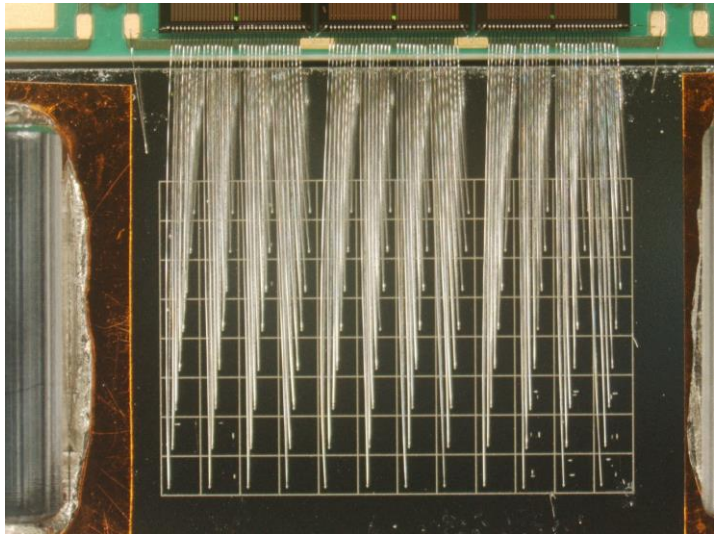

Complete detector system with closed cycle cryostat

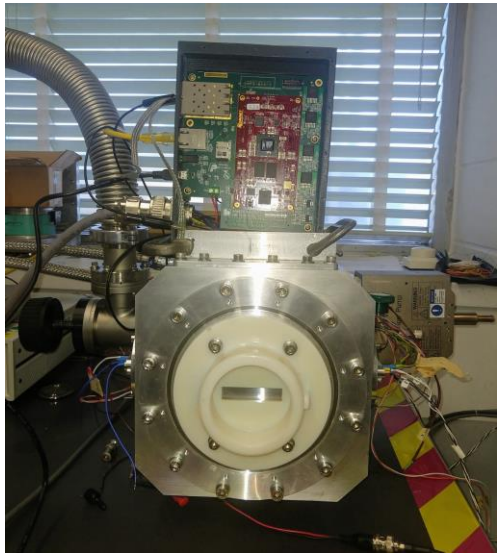

Response from Fe55
Resolution ~280 eV

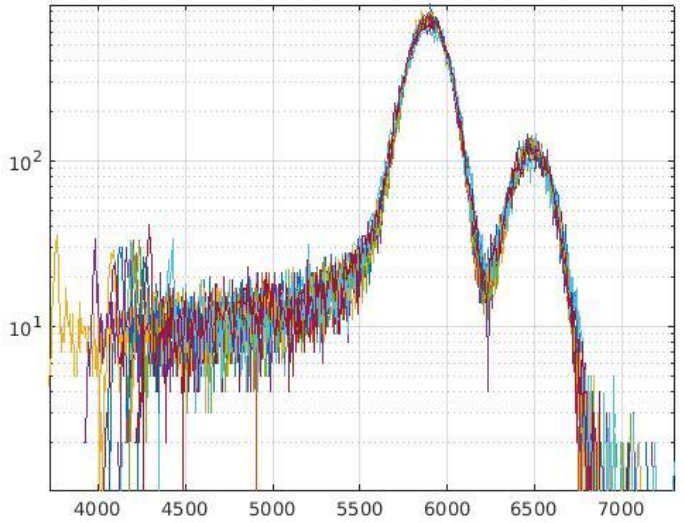

Single pixel response from Co57

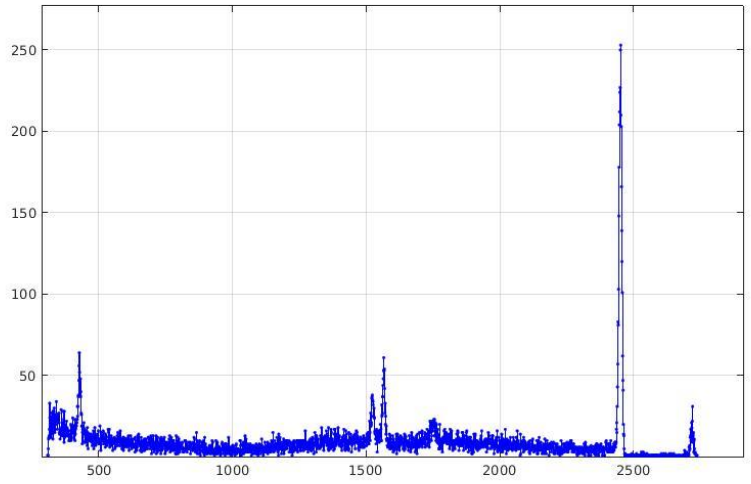

Resolution from Co 57
~720 eV at 122 KeV

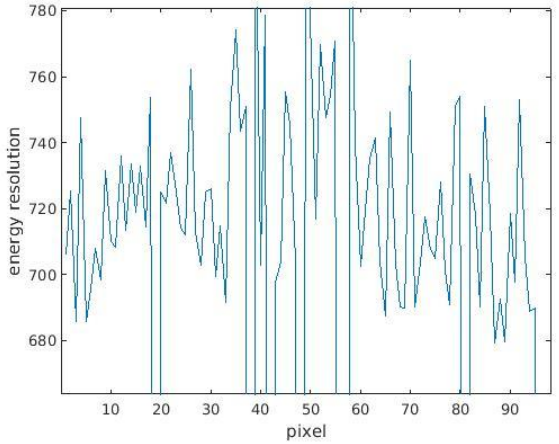

Plan for 384-Germanium Maia detector
Left: drawing of the sensor mount and cold head
Right: 384-Gaia sensors

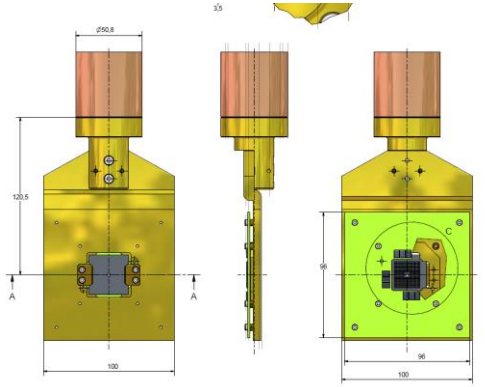

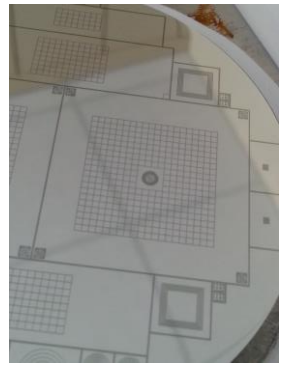

Germanium Drift Detector (GDD)

- Silicon drift detector offers the best energy resolution. Invented by Gatti and Rehak at BNL.
- Uses long lifetime and high mobility of charges in depleted silicon to reduce capacitance of collection electrode.
- Planar Germanium version of drift detector not made yet. Fabrication challenges

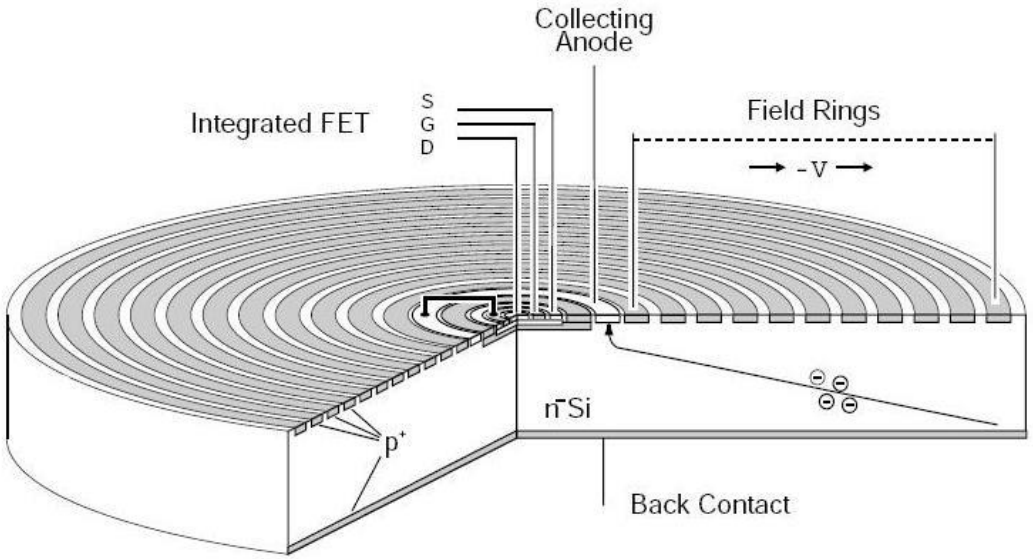

Germanium Drift Detector (GDD)

Cryostat and sensor cooling design currently underway

Read out with Cube pre-amp.

Sensor characterization would be done with cryogenic probe station

Stay tuned for more results!

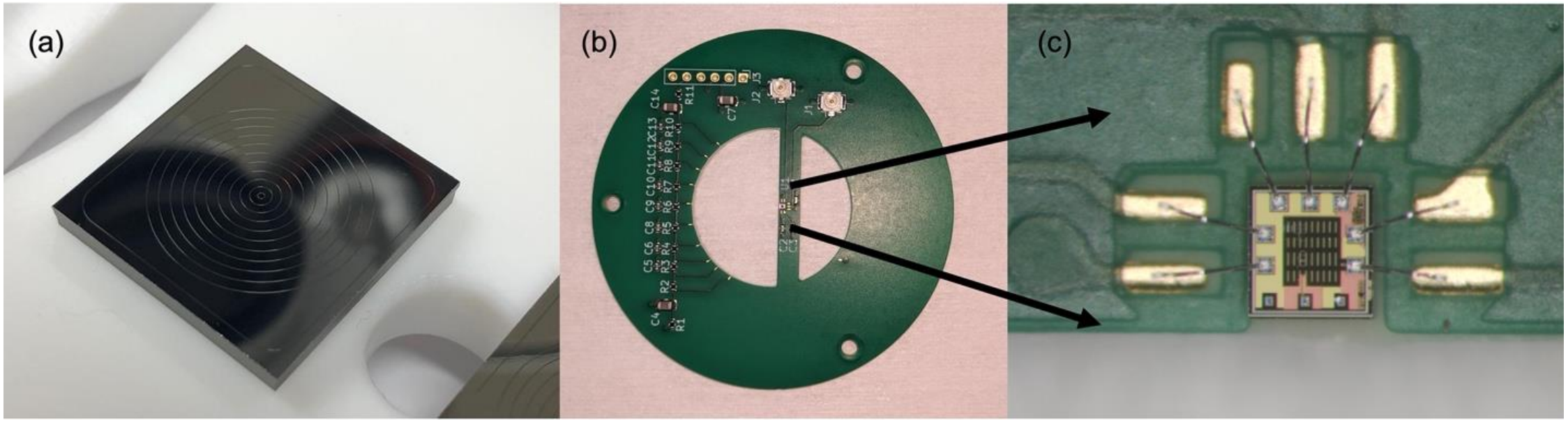

Amorphous Selenium for Medical Imaging

Amorphous Selenium

- The most prevalent commercial detector for low-light detection with high dynamic-range and linear-mode operation is the vacuum photo multiplier tube (PMT).
- Bulky and fragile, have poor quantum efficiency in the visible spectrum, are insensitive to infrared light and highly sensitive to magnetic fields.
- Amorphous Selenium (*a*-Se) is emerging as a viable solid-state imager with avalanche gain for low light and low-dose radiation detection applications.

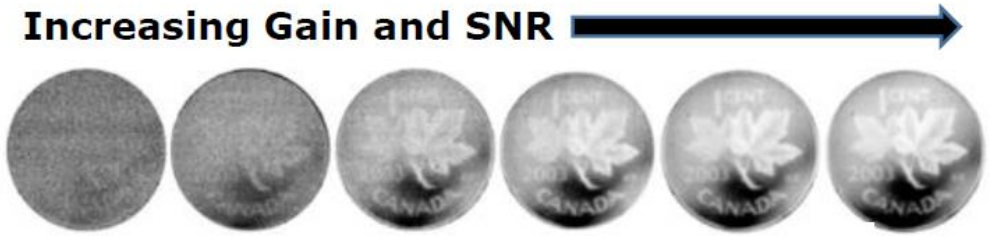

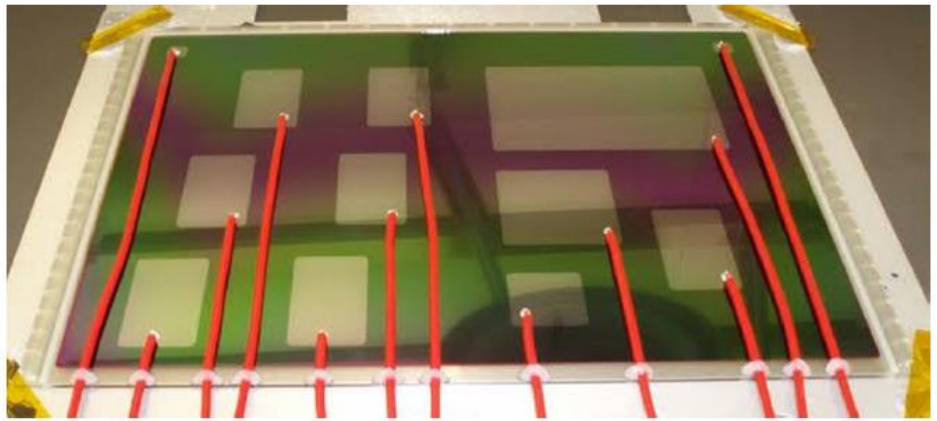

Figure: Si TFT array covered with a continuous layer of avalanche *a*-Se detector (24 cm x 30 cm). [1b]

1b. J. Scheuermann et al. *In: Med. Phys.* (2018).

a-Se: Advantages & Challenges

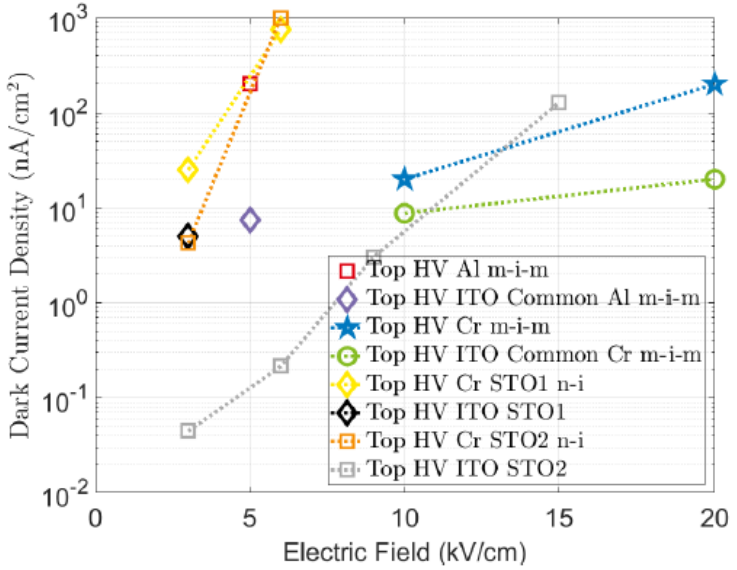

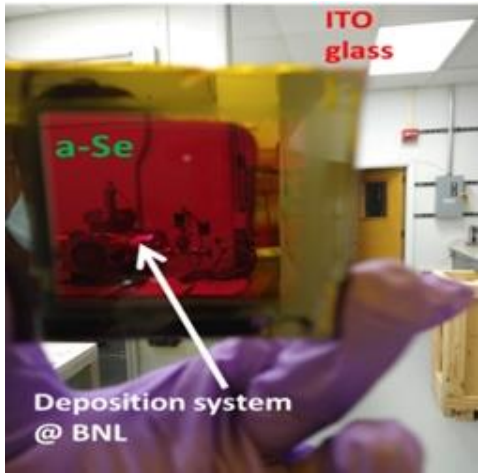

- Amorphous Selenium is commercially used as a direct conversion X-ray and Gamma ray detector for digital radiography and mammography.
- It can be deposited uniformly over a large area at substantially lower costs as compared to crystalline semiconductors.
- High spatial resolution (below 10 microns) can be achieved for hard X-rays.
- Carrier mobility is poor
- W is high & field dependent

Brookhaven National Laboratory

Fabrication- Pad Extension

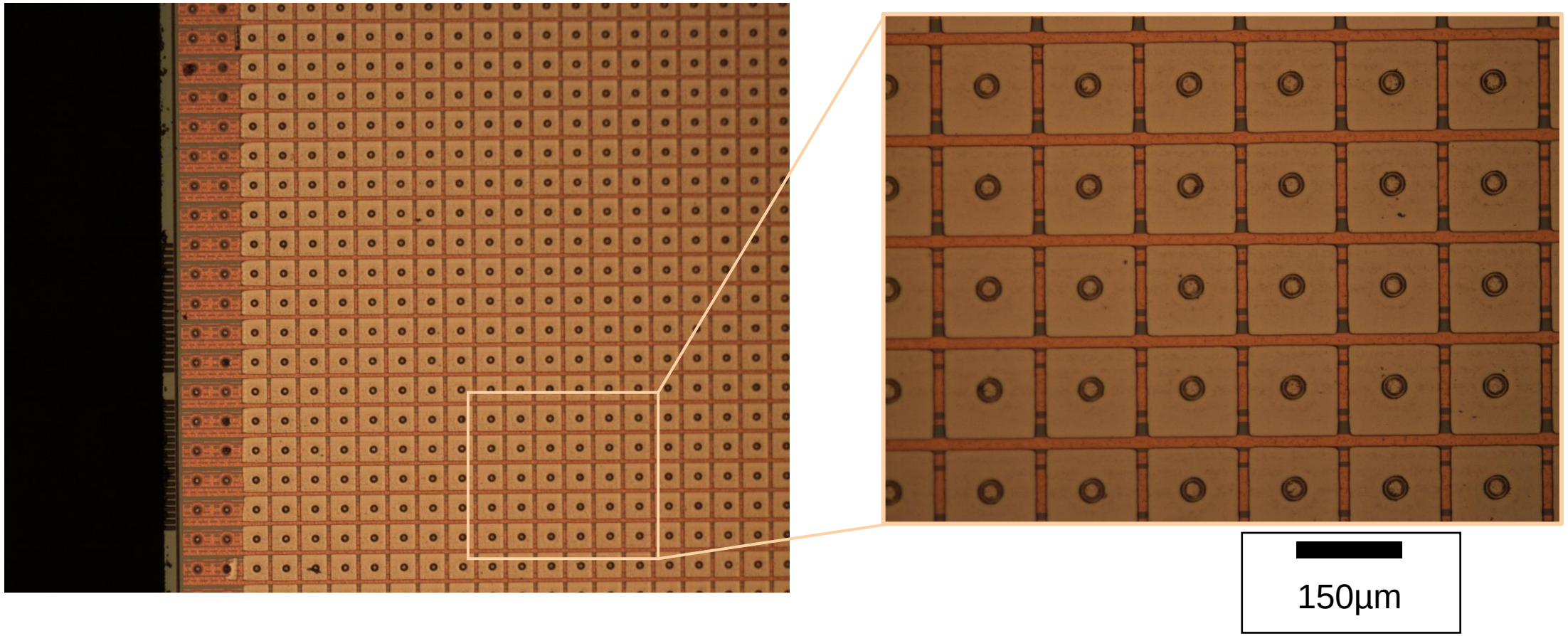

After Liftoff

Fabrication- rest of the detector

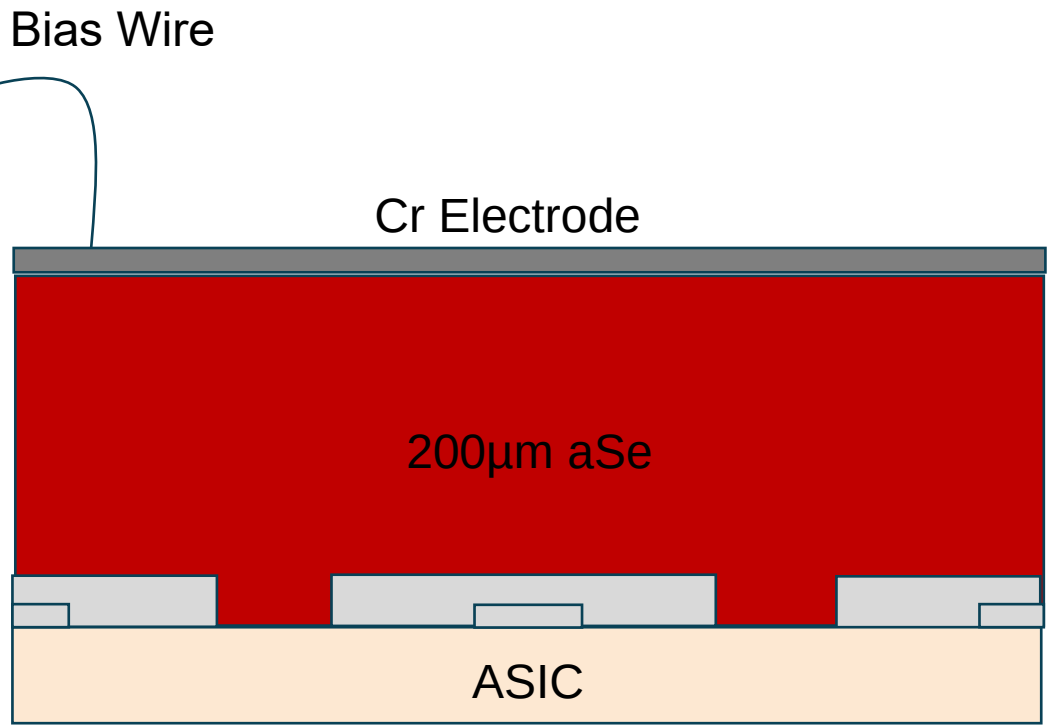

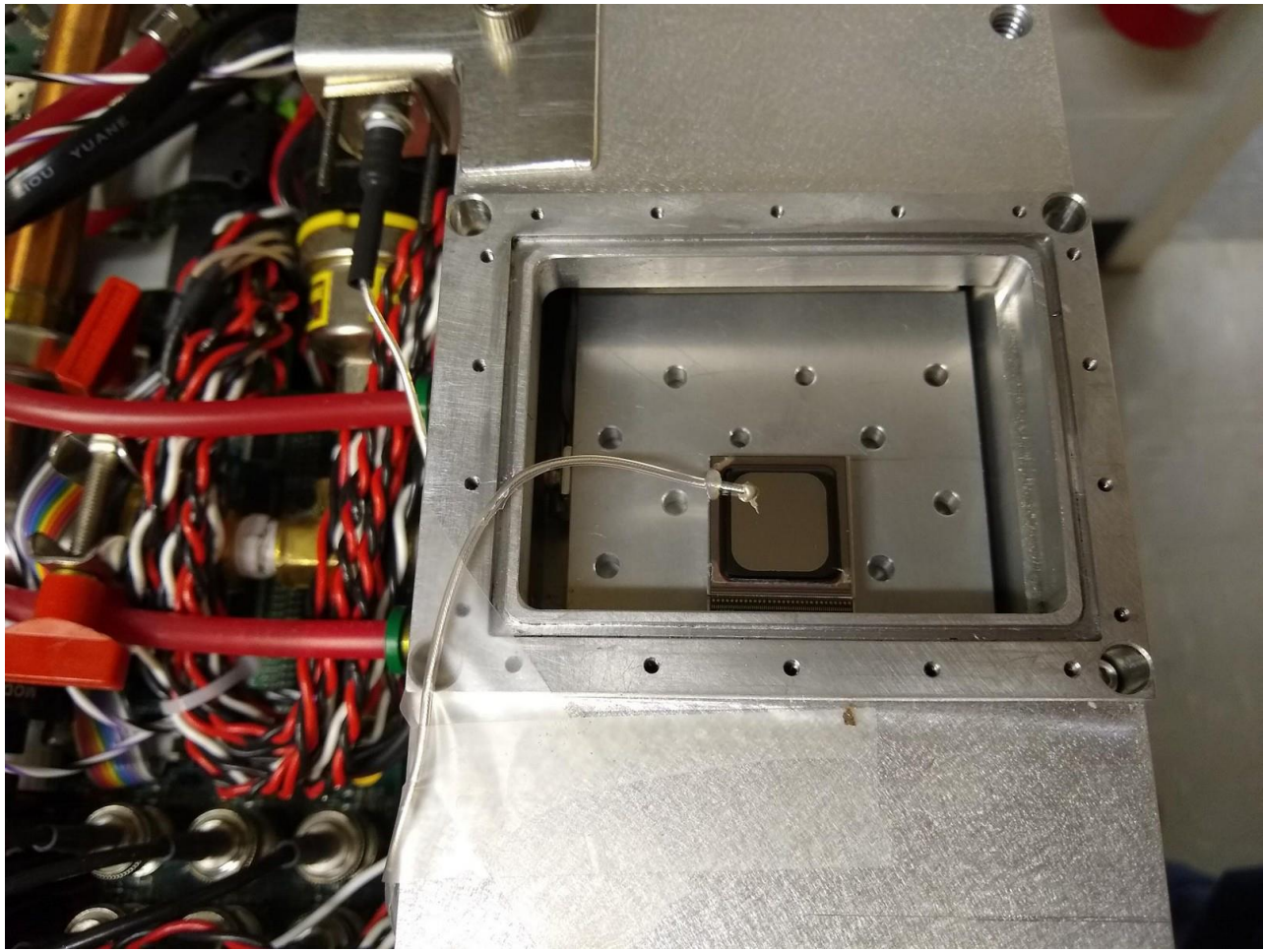

Initial Tests

1.6% rms variation

- Ag x-ray tube, 45 kV bias
- Average of 100 frames, 100ms exposure each

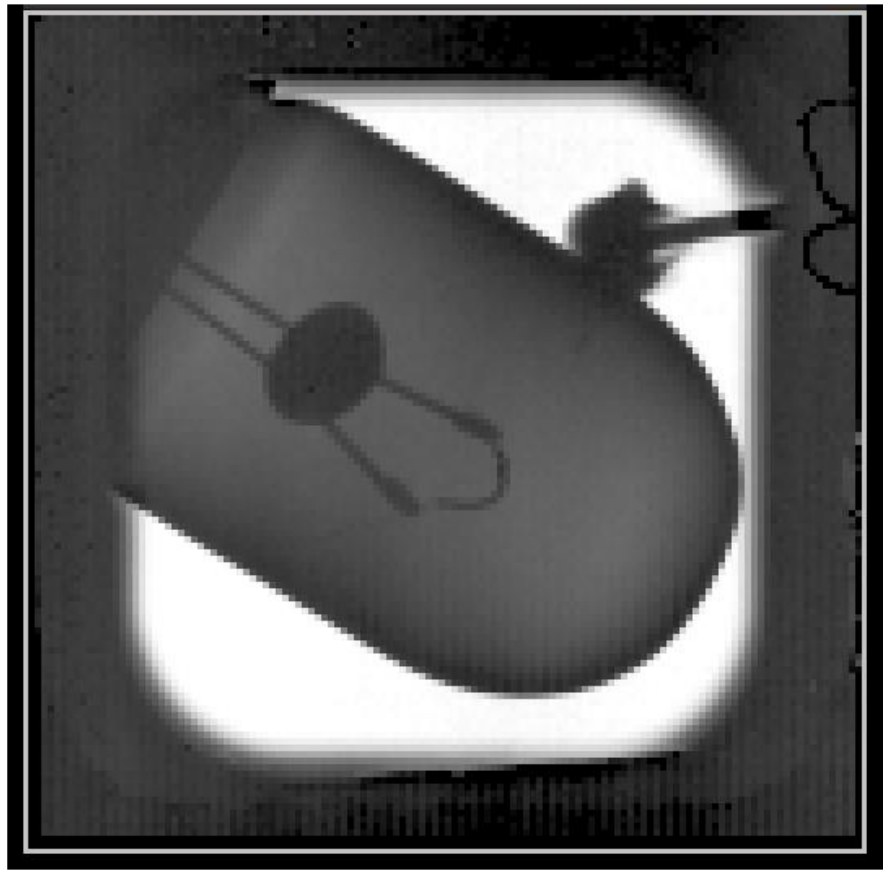

Image of lightbulb, raw data (no flat field)

Brookhaven National Laboratory

Dynamic Response

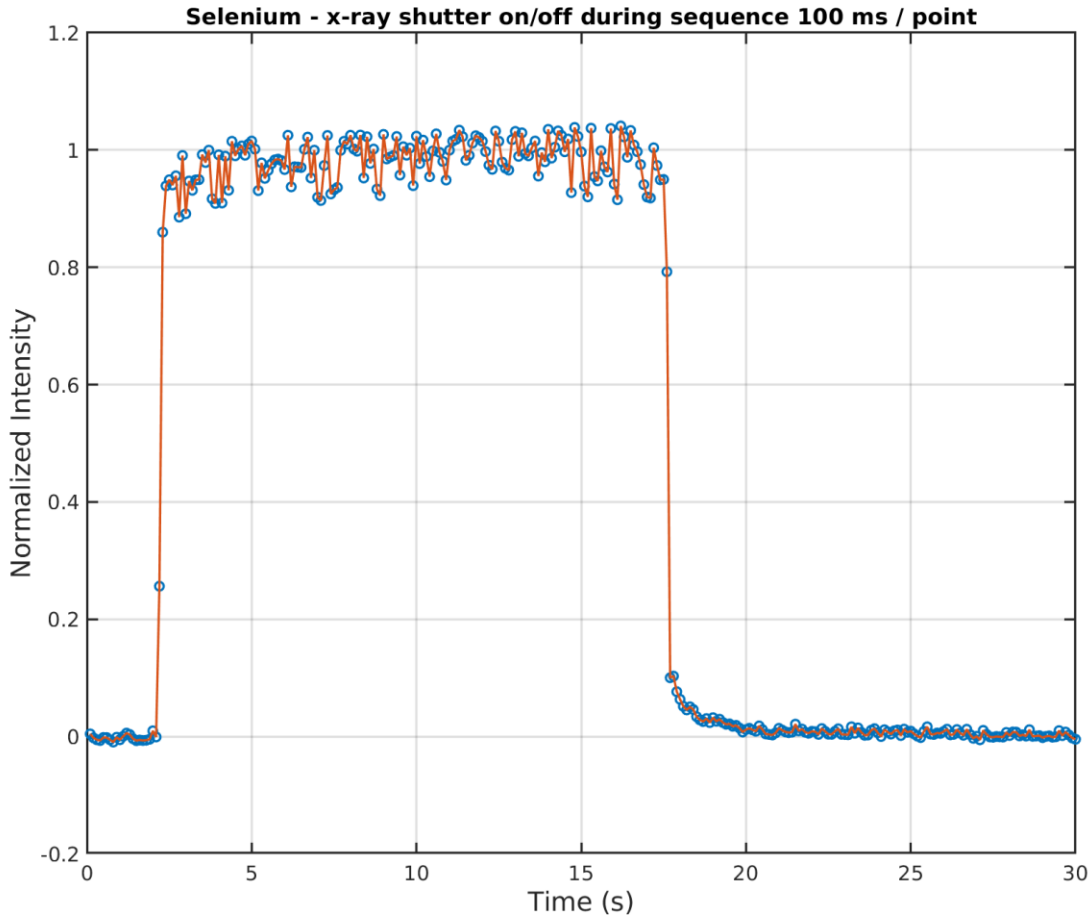

Static knife edge, shutter opened and closed

-100ms

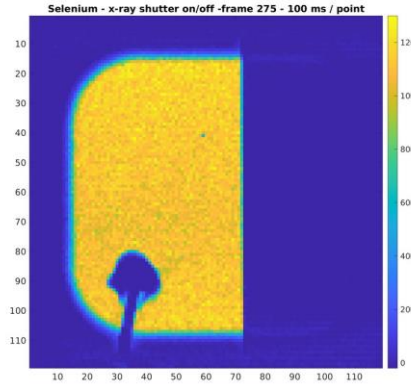

0ms

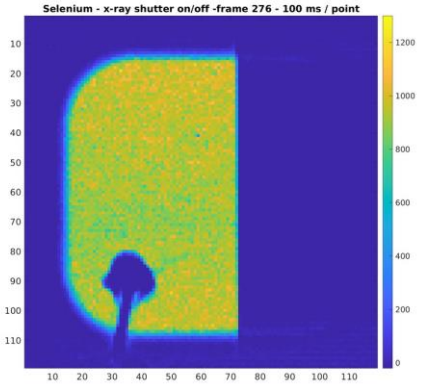

100ms

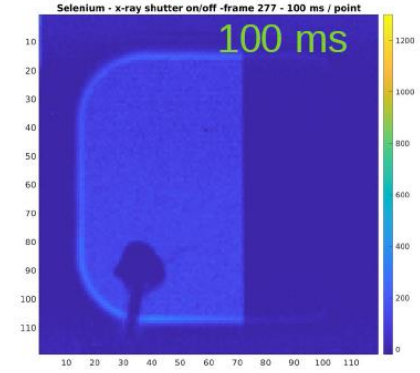

400ms

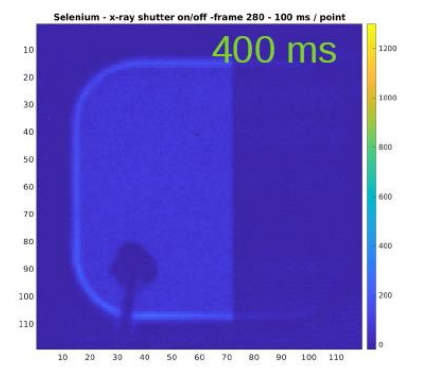

1400ms

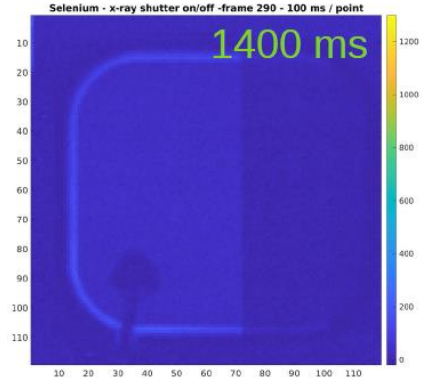

2400ms

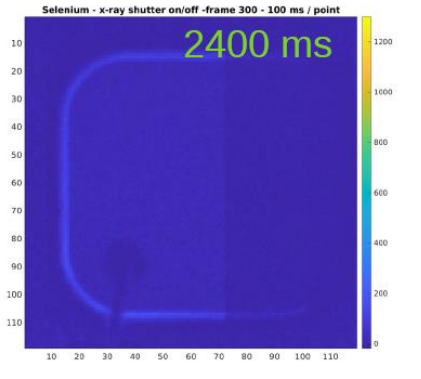

Brookhaven National Laboratory

Knife Edge at an Angle

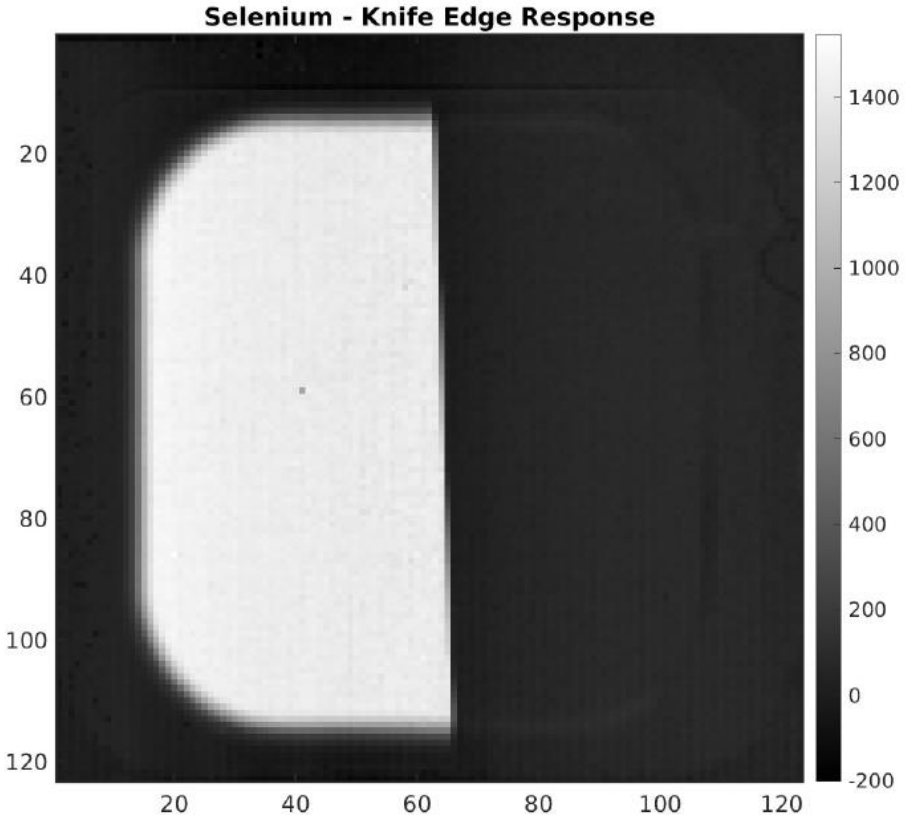

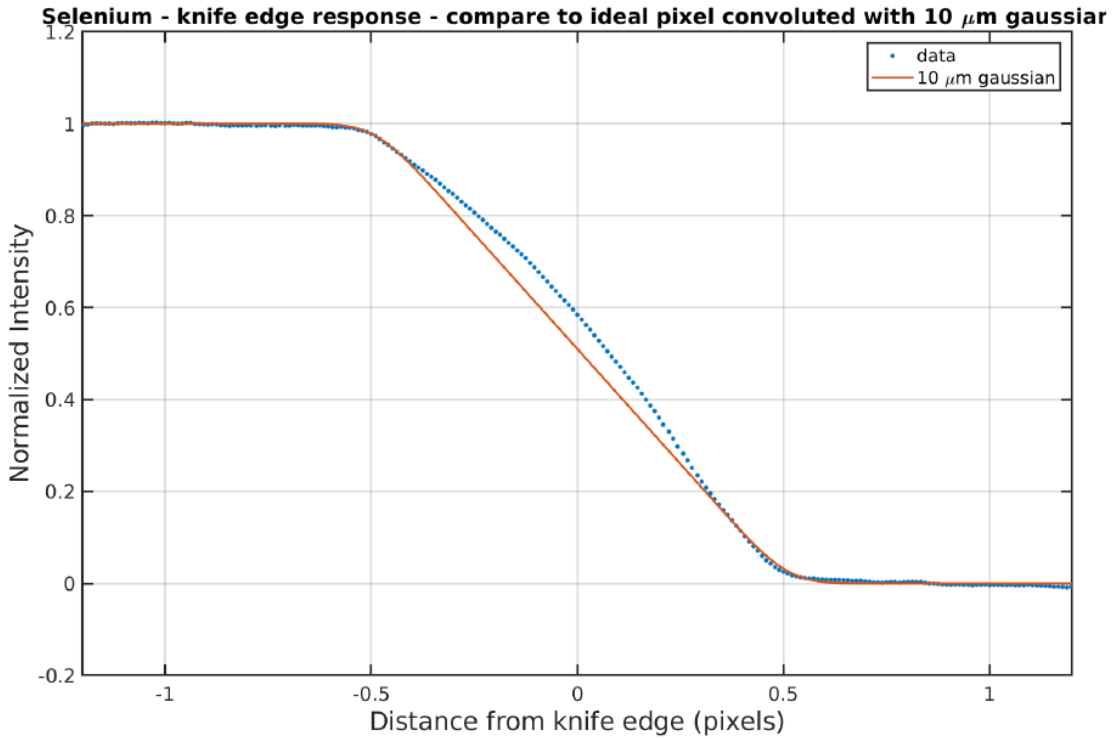

Deviation from ideal response- more intense than expected

MTF for different energies

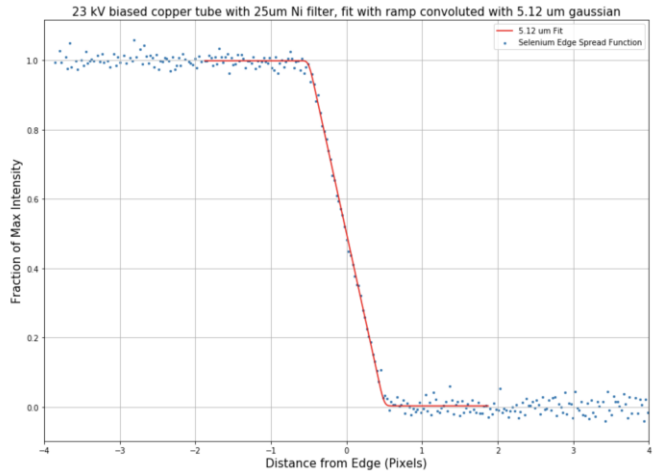

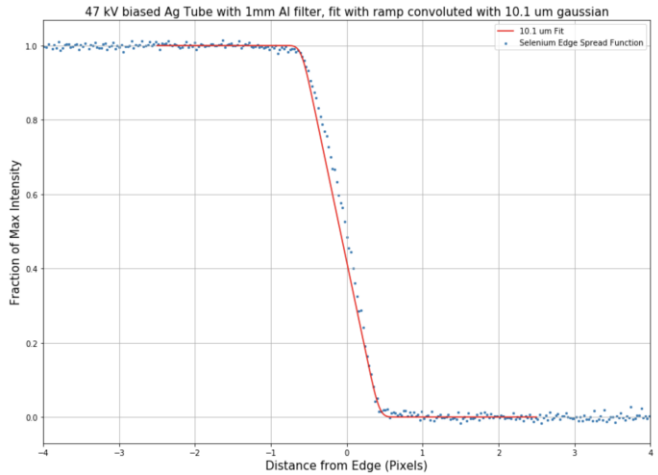

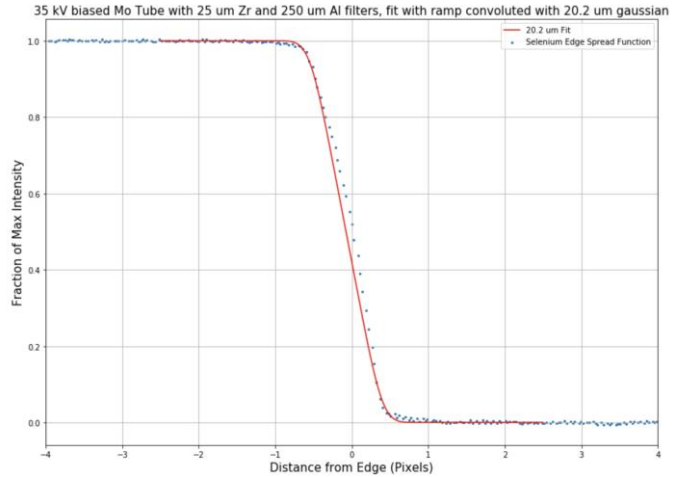

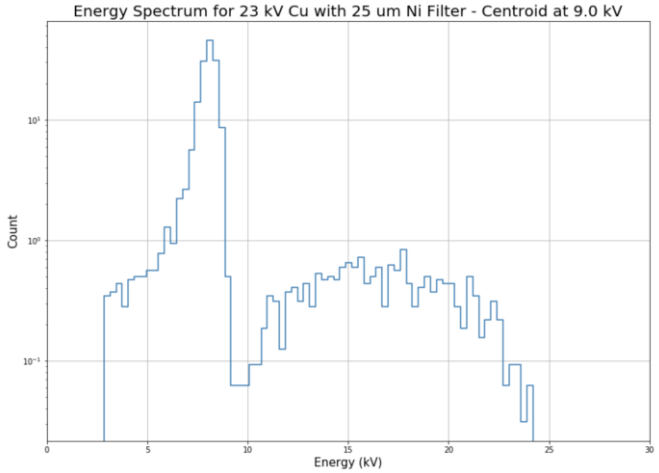

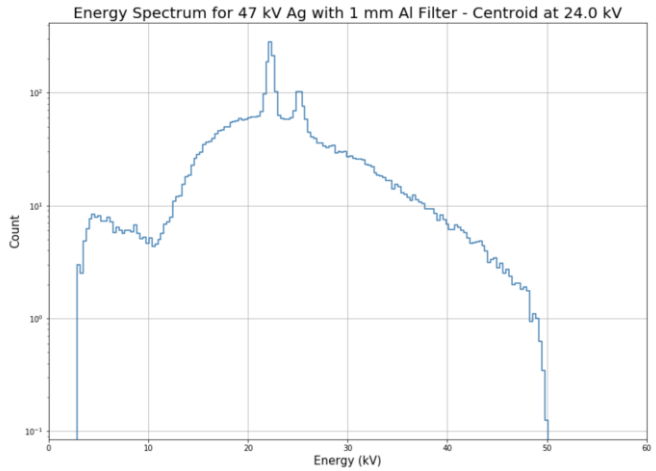

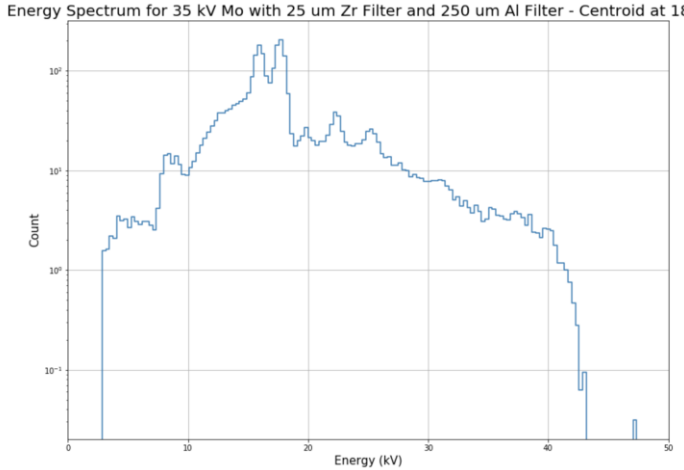

Brookhaven National Laboratory

Simulation of intrinsic spatial resolution

Semiclassical Monte Carlo Boltzmann Transport equation

$$\frac{\partial f_{\mathbf{k}}(\mathbf{r})}{\partial t} + \frac{\mathbf{F}}{\hbar}.\nabla_{\mathbf{k}} f_{\mathbf{k}}(\mathbf{r}) + \frac{1}{\hbar}\nabla_{\mathbf{k}} E_{\mathbf{k}}.\nabla_{\mathbf{r}} f_{\mathbf{k}}(\mathbf{r}) = \frac{\partial f_{\mathbf{k}}(\mathbf{r})}{\partial t}\Big|_{\text{coll}}$$

- Transport of holes interrupted by acoustic, polar and non-polar phonons, disorder, and dipole scattering
- DFT used to calculate energy dependent phonon scattering, dipole and disorder scattering
- Transport model validated with experimental data i.e time-of-flight mobility and impact ionization gain

Brookhaven National Laboratory

A. Mukherjee et al. JAP, 124, 235102, 2018

Simulation of intrinsic spatial resolution

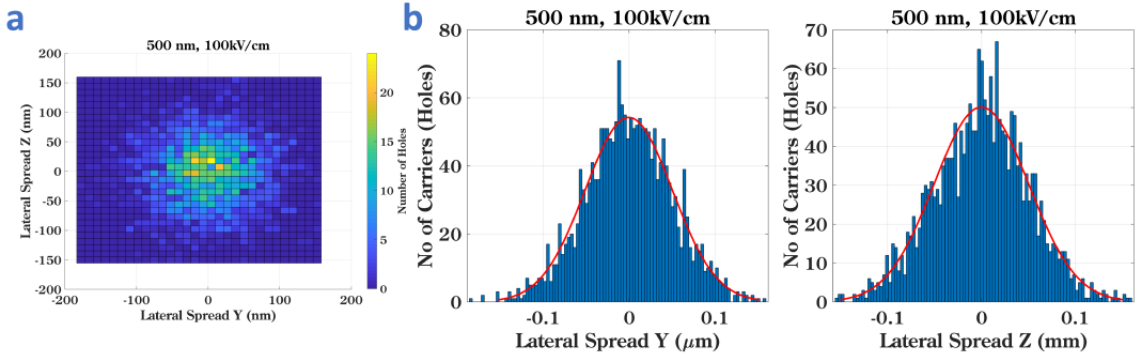

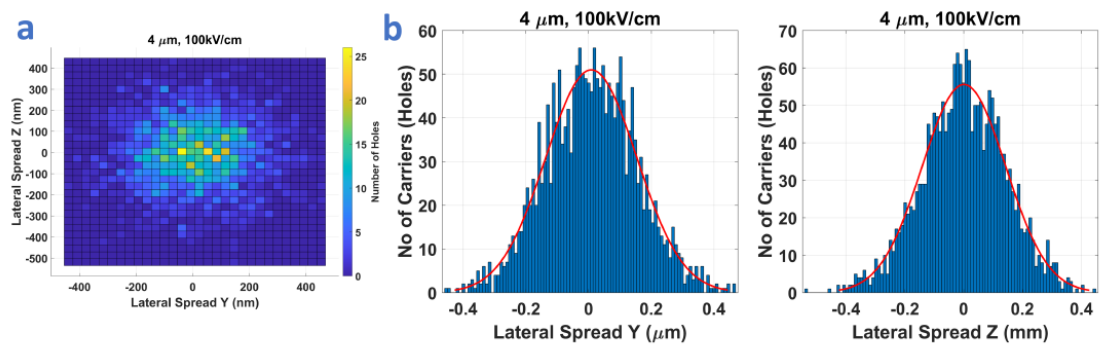

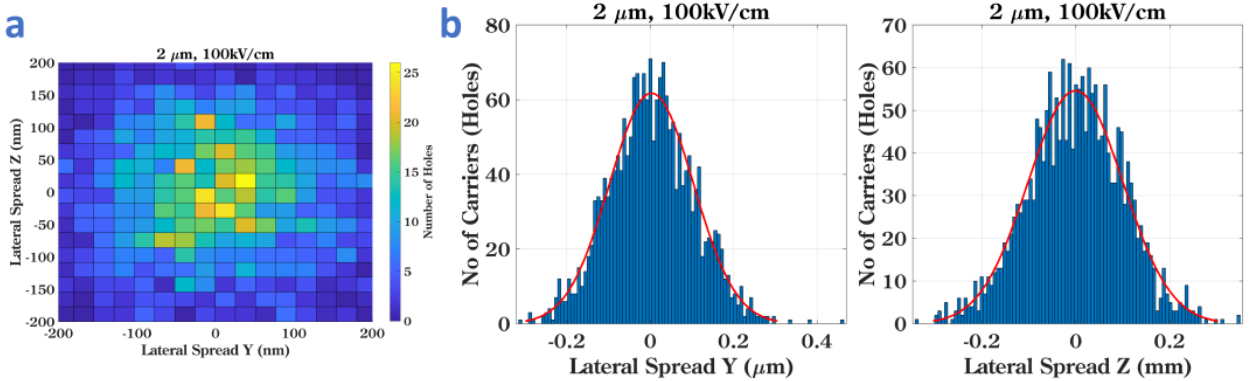

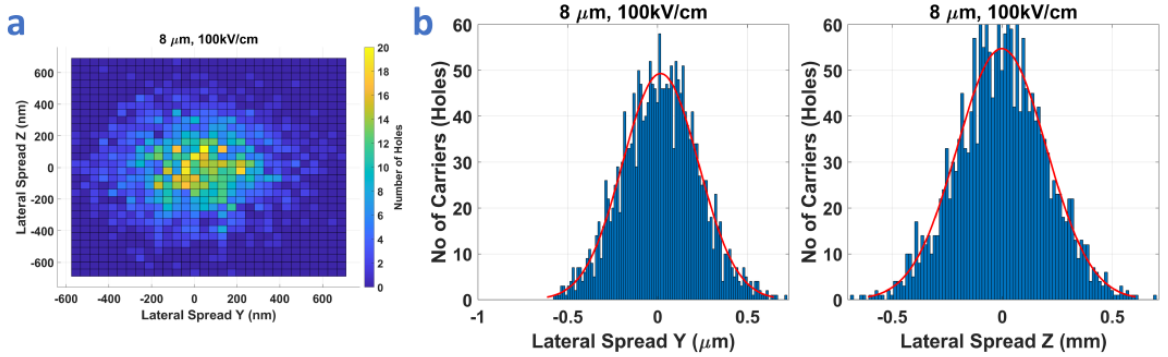

Intrinsic MTF for 200-micron Se was about 2.5 microns

Brookhaven National Laboratory

field-Shaping multi-Well Avalanche Detector

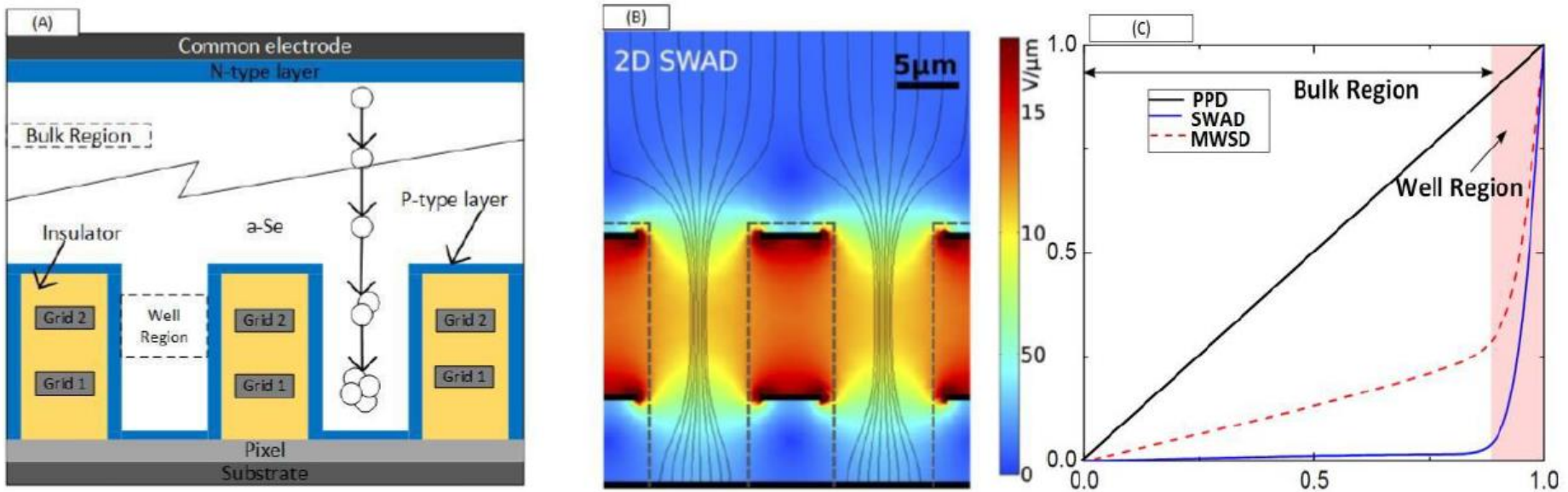

- **Can address the problem of low carrier mobility and low charge conversion gain by having a Frisch Grid built in the sensor layer.**
- Uniform gain, independent of depth of interaction.
- Reduced charge collection time.
- Leakage in the well has to be minimized. Leakage limits gain.
- Non-trivial fabrication process.

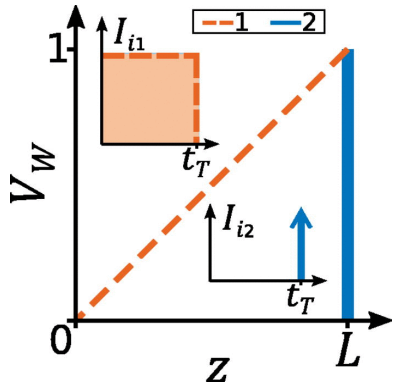

Appl. Phys. Lett. **101**, 213503 (2012)

Future research in a-Se - SWAD with high-k hole blocking layer

- Fabrication of field-Shaping multi-Well Avalanche Detector (SWAD): Improving time resolution and uniformity in gain

The schematic diagram of SWAD design

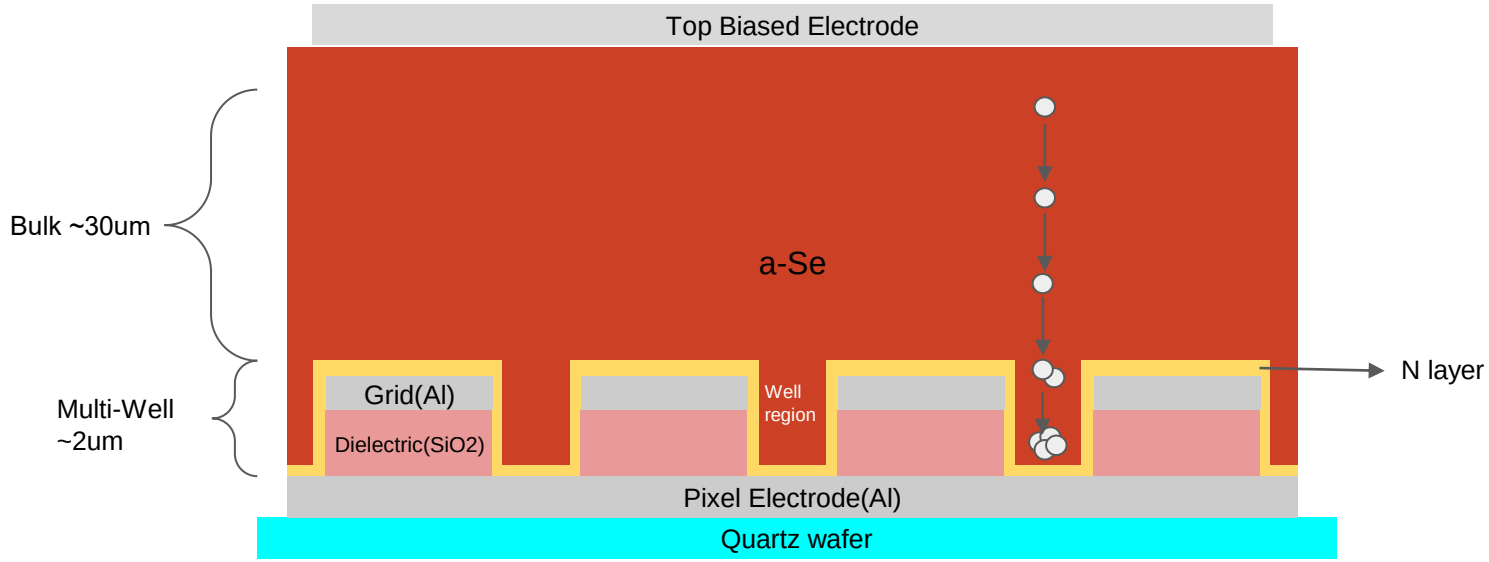

SWAD with hole blocking layer

Fabrication

The illustration of fabrication process steps to fabricate SWAD multiwell structure, utilizing photolithography, Reactive Ion Etching(RIE), and material deposition techniques

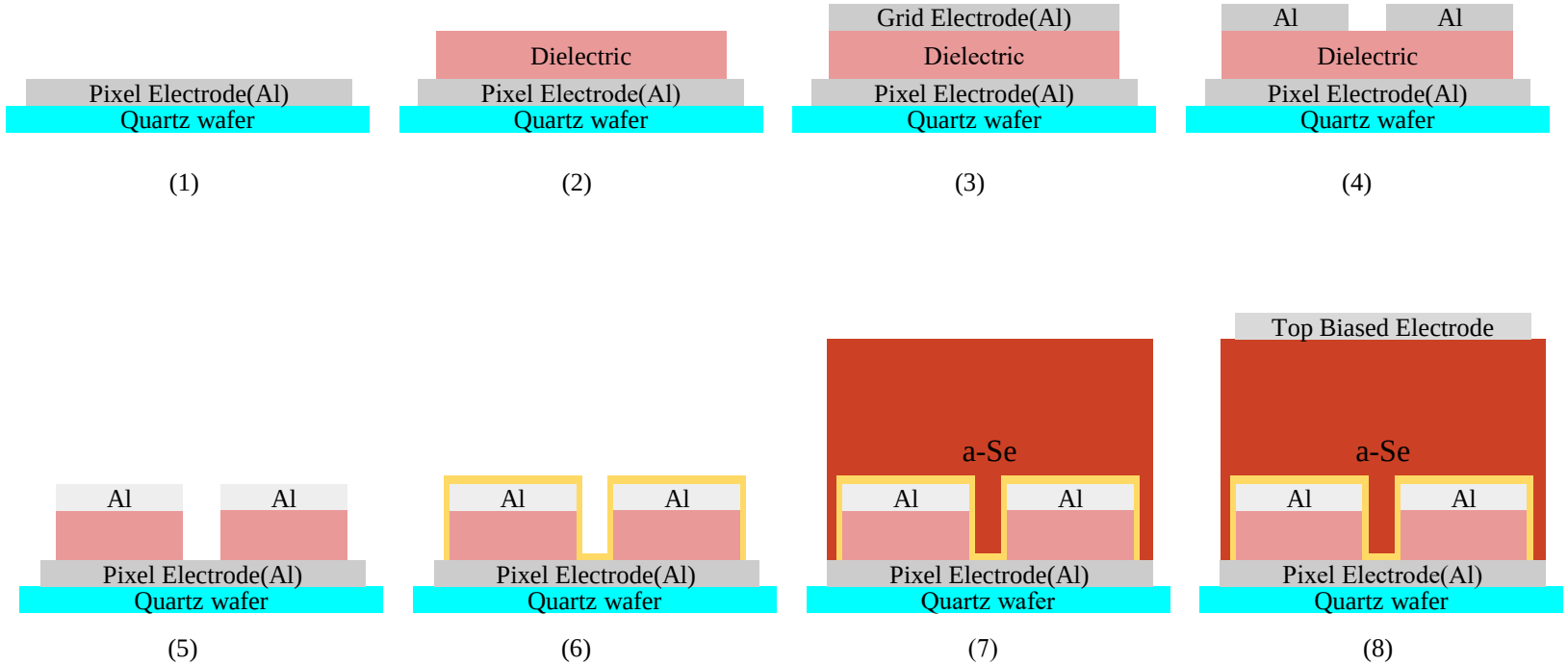

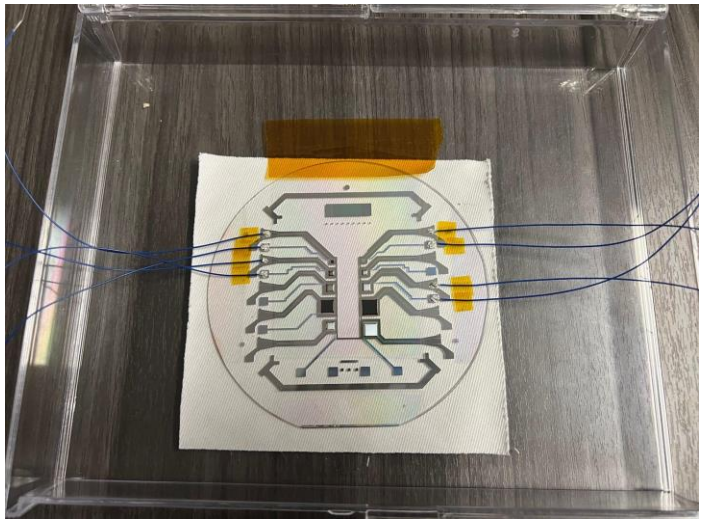

Large band gap semiconductor

Diamond

Cubic $F\bar{d}3m$ space group
Band Gap: 4.11 eV

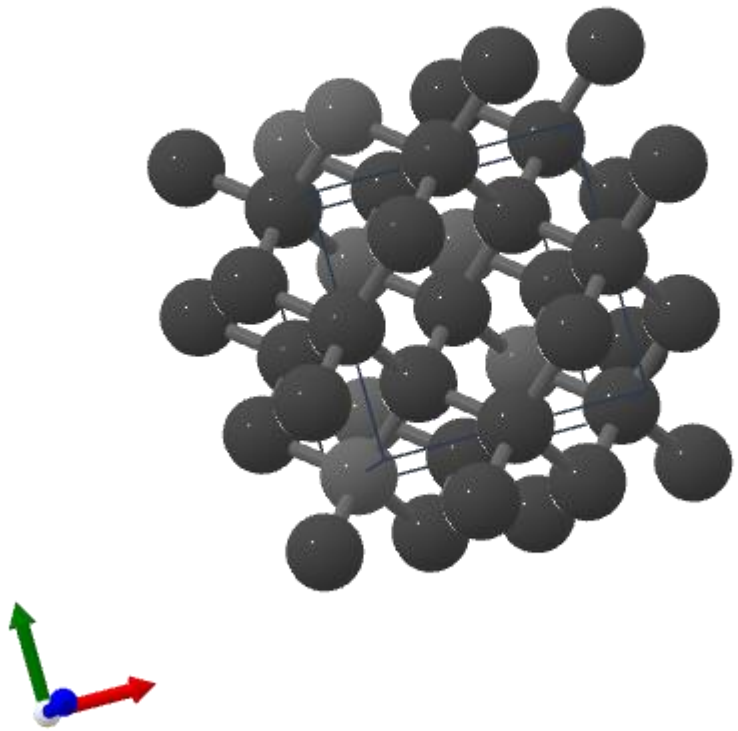

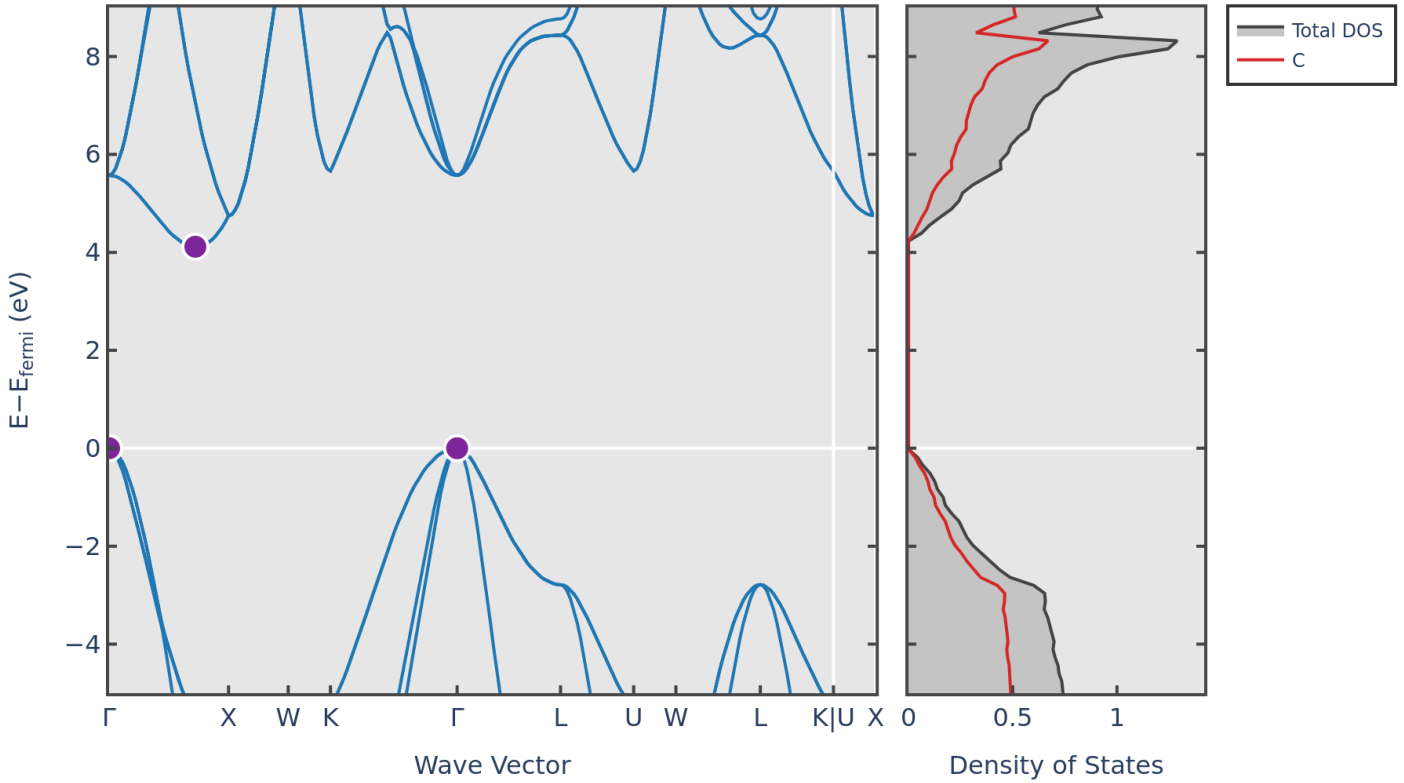

Brookhaven National Laboratory

Diamond detector Work at Instrumentation Division, BNL: Erik Muller

Why diamond

Benefits of diamond

- Large band-gap: low leakage, high resistivity
- Radiation hard
  - Damage appears as reduction of signal
  - In silicon, there is potential for both signal reduction and increased leakage
- Higher saturation velocity
  - Diamond: 2.7×10^7 cm/s (e)
  - Silicon: 1×10^7 cm/s (e)
  - Transit time for a 50 µm-thick device: 185 ps (diamond), 500 ps (silicon)

Challenges of diamond

- Cost/availability
- Size
  - Single crystal material is limited to 4.5 mm × 4.5 mm
  - Polycrystalline diamond available 1 cm x 1 cm
  - Requires a tiling solution which complicates assembly
- Higher W than silicon – about 1/3 lower signal

Diamond - Detector

Ionization energy

13.3 eV

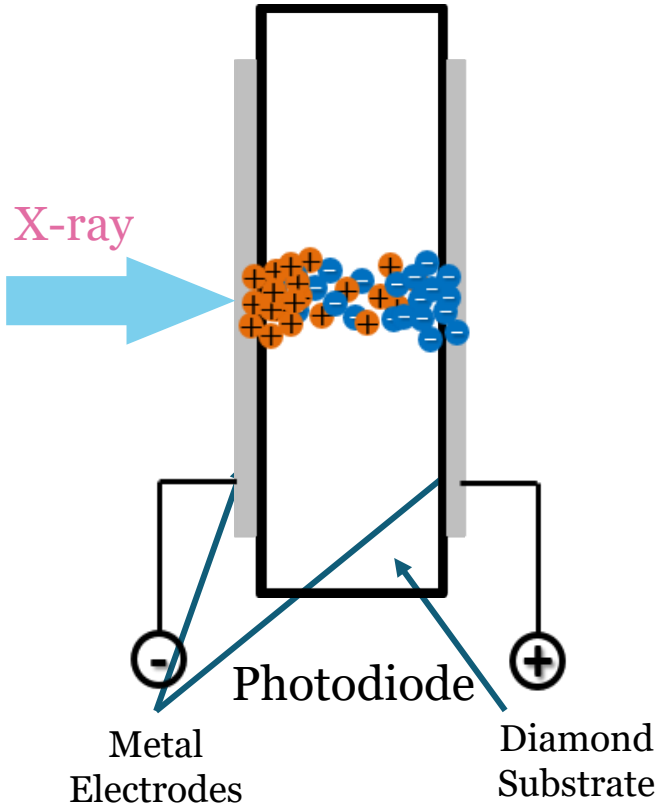

Two Scenarios

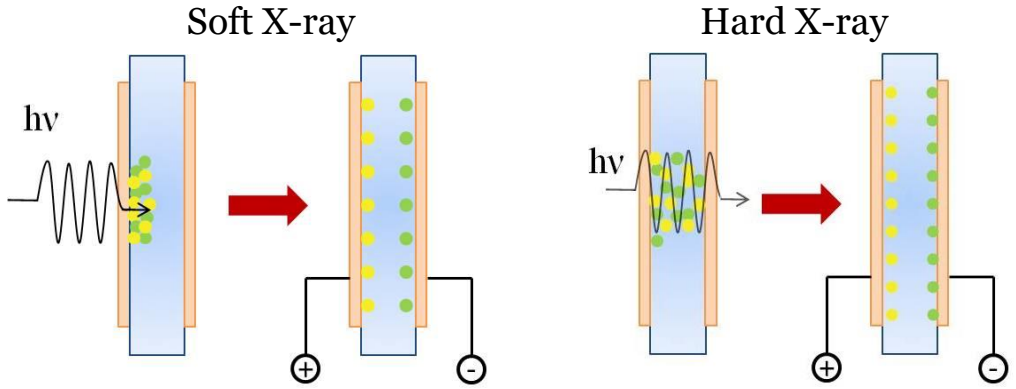

Attenuation Length

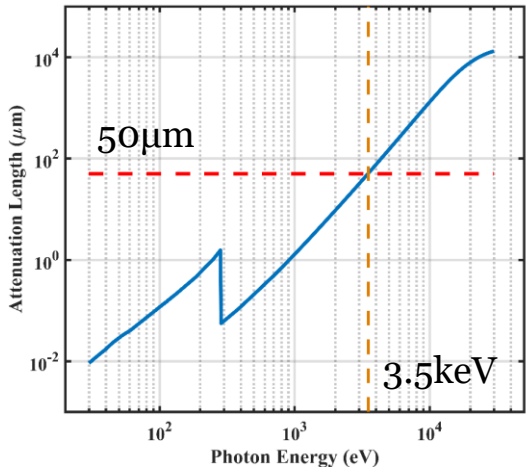

Transmission Ratio

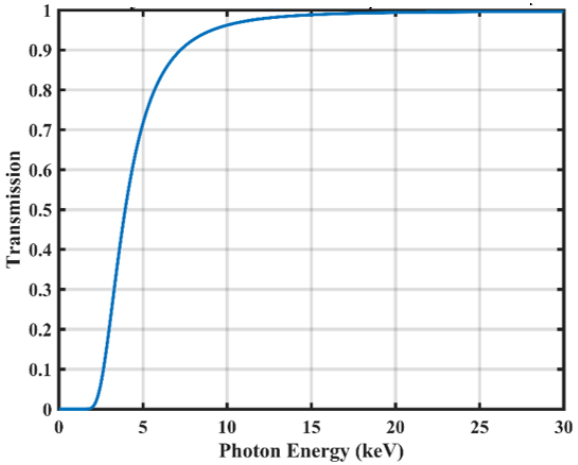

Brookhaven National Laboratory

Diamond Imaging Detectors

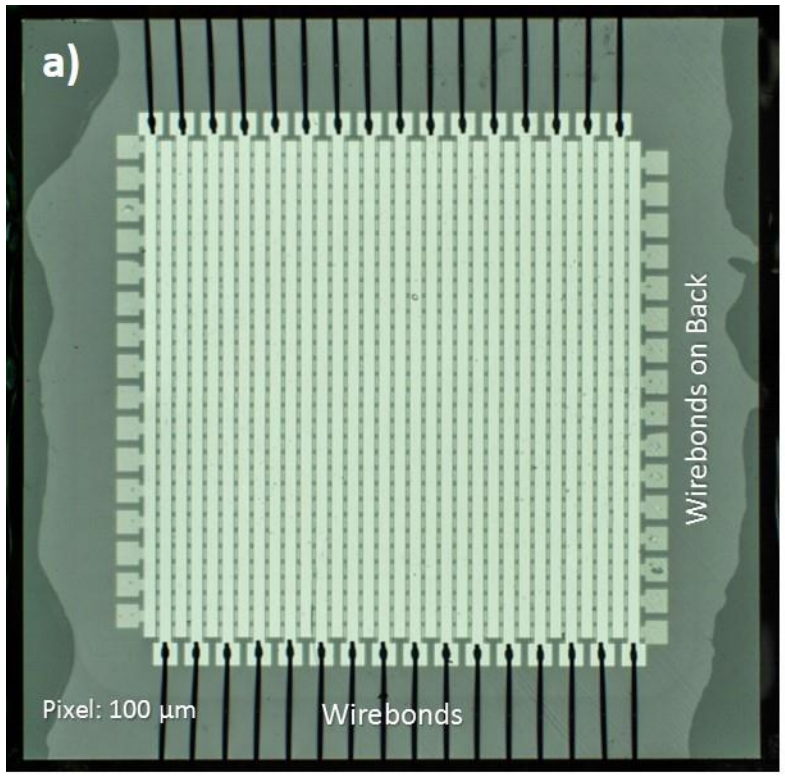

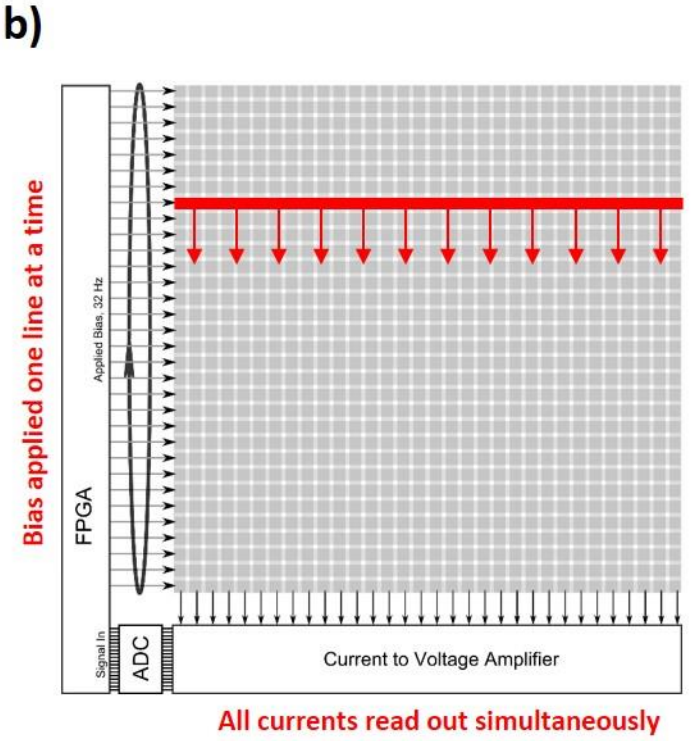

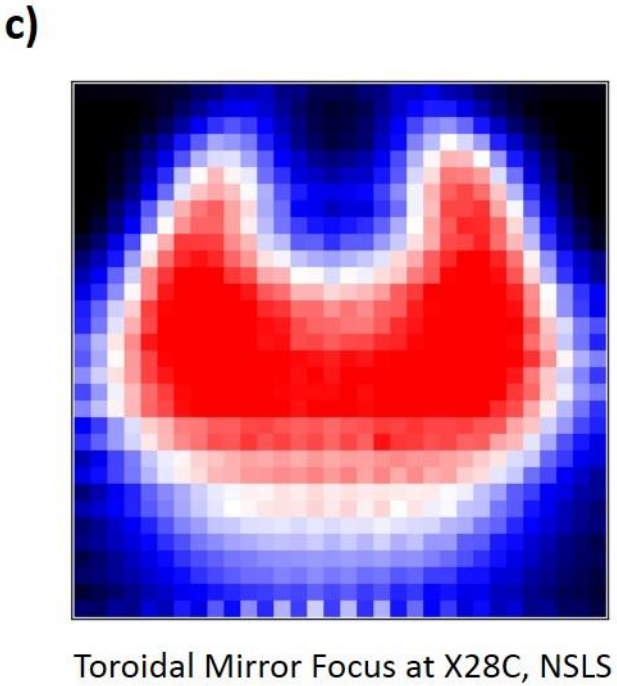

Diamond imaging detector. (a) A diamond sensor with 20 nm-thick platinum strips forming 100 µm virtual pixels. (b) Readout scheme where the bias is applied to individual strips to read out the one line at a time. A complete image is readout out at ~32 Hz. (c) image of white x-ray beam after a toroidal focusing mirror.

CdZnTe for Gamma Rays

Advantages of Cadmium Zinc Telluride (CZT) Material

- High average Z
- High density (g/cm^3)
- Wide bandgap → high-resistivity
- → can operate at room temperature;
  (best results usually obtained at ~5-10 C)
- Provide high energy resolution (sub keV in X-ray region, and ~1% at 662 keV in gamma-ray range) and sub-millimeter spatial resolution for imaging devices
- Device fabrication utilizes technologies developed in semiconductor industry, which make CZT detectors less expensive and more robust
- CZT is very attractive material for gamma-ray detectors; Its feasibility has been demonstrated in many applications
- However, crystal defects, which exist even in the best quality CZT crystals, limit availability and increase costs of CZT detectors; the main challenge facing today detector developers is how to overcome these problems

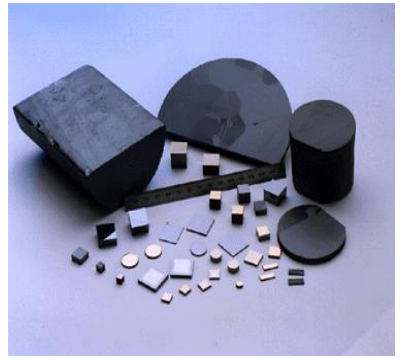

Why do we need to detect gamma rays?

- Gamma rays emitted by radioactive nuclei and unavoidably present in our environment
- Provide unique signatures of isotopes and nuclear reactions taking place at nature
- Gamma rays are emitted at discrete energies seen as peaks in their energy spectra
- Because the natural widths of the peaks are very narrow they are called gamma-ray lines
- Energy spectra can be used like ID cards to identify particular nuclei

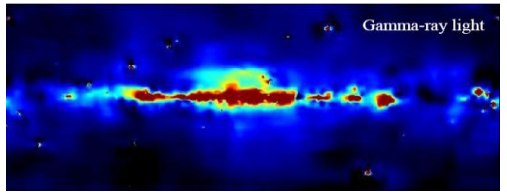

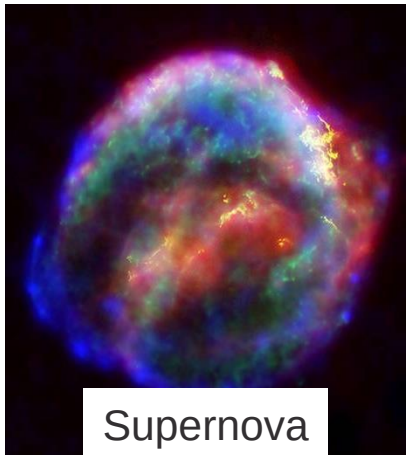

Supernova

Example of ideal gamma-ray energy spectrum

Lines indicate intensities and energies of gamma-rays

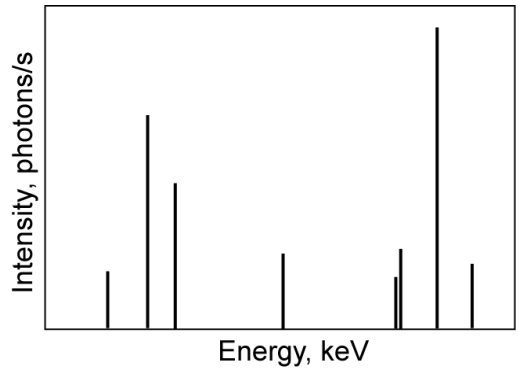

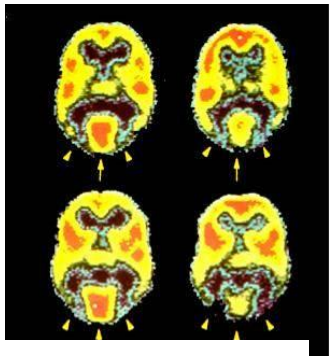

PET scan image

Nuclear reactor

Brookhaven National Laboratory

CZT growth techniques

There are two major producers of commercial detector-grade CZT material: eV Products (USA) and Redlen (Canada)

They can grow relatively big single crystals, up to 10 of cc

For a while eV-Products and Redlen used different growth methods:

High-Pressure Bridgeman (eV)

~1100 C,

Use high-pressure nitrogen gas to suppress formation of point defects

Best quality CZT small-size crystals

Very non-uniform on a large scale (extended defects)

Wafer cut from a 7-inch ingot

Traveling Heater Method (Redlen)

~600 C

Very uniform

Quality to satisfy requirements for making detectors

Lower cost

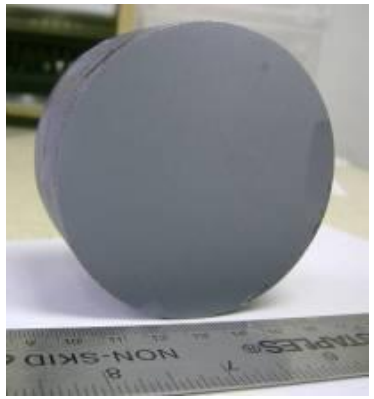

3-inch wafer

Novel CZT instruments based on arrays of position-sensitive virtual Frisch-grid detectors

Solid shieling electrode (conventional)

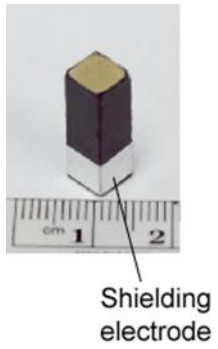

Position-sensitive virtual Frisch-grid detector

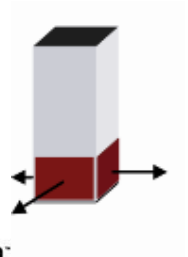

- To overcome the high cost and low availability of big CZT crystals we propose arrays of small cross-section, up to 7x7 mm^2, but long, up to 5 cm, detectors
- Such crystals have much higher production-yield and lower; typically cut from the crystals rejected by other costumers
- 4 position-sensing pads (non-contacting electrodes) attached to the side surfaces near the anode; the pads signals provide X-Y coordinates
- The cathode signals are used to measure drift times to evaluate Z coordinates, like in TPC;
- C/A ratio gives independent estimates for Z
- Virtually grounded pads produce the Frisch-grid effect (as if a real grid were placed inside the detector)

This design (drift cell) was originally proposed for noble gas detectors by V. Dmitrenko et al. This idea was later applied to CZT detectors by G. Montemont (LETI) and D. McGregor (Kansas State University)

CZT bars

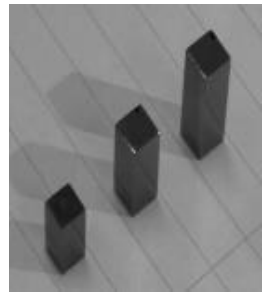

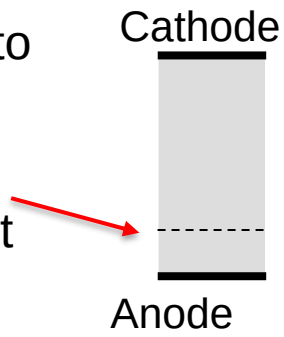

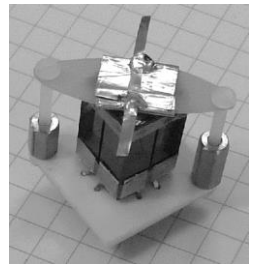

Brookhaven National Laboratory

CZT (Redlen) sensors bonded to readout chip

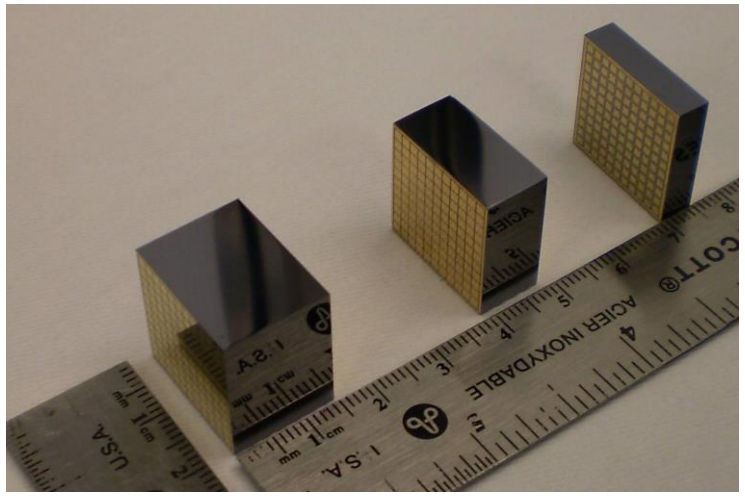

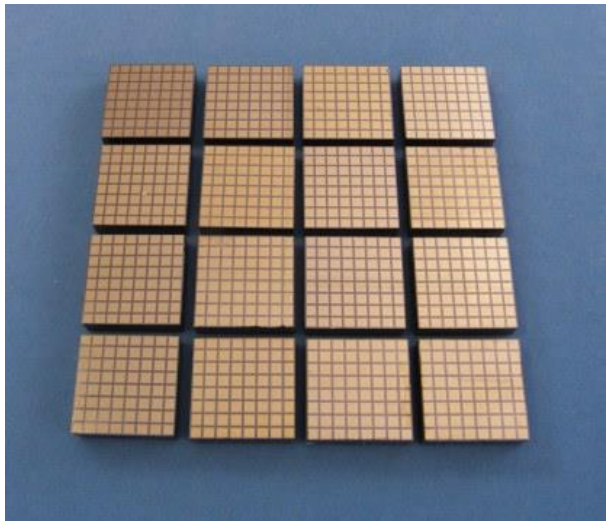

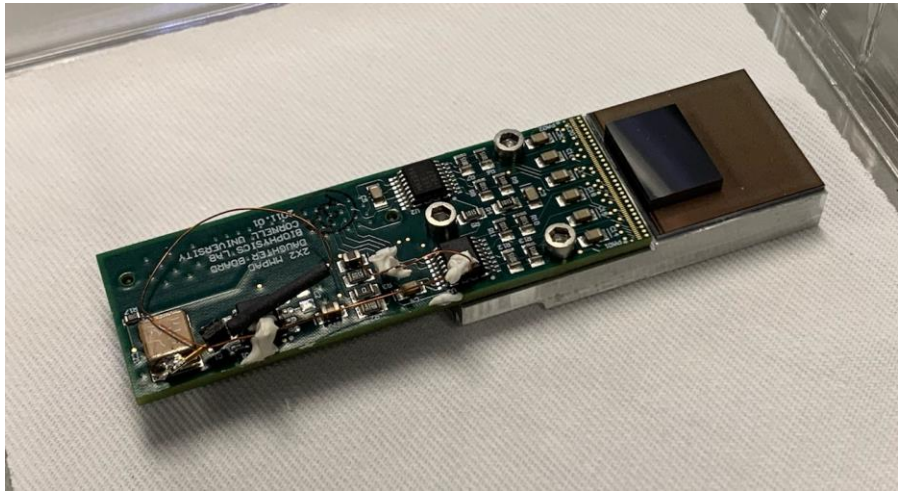

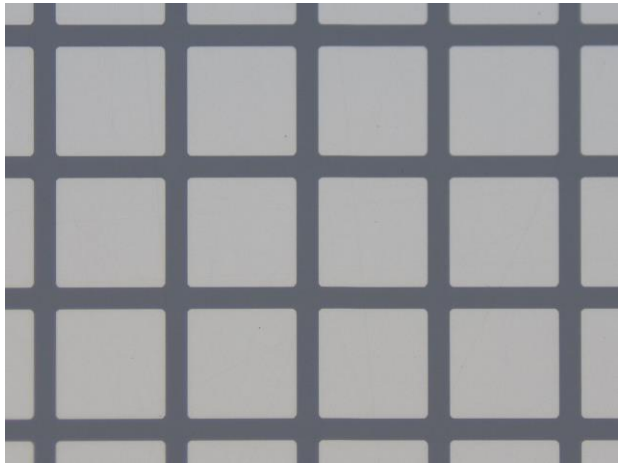

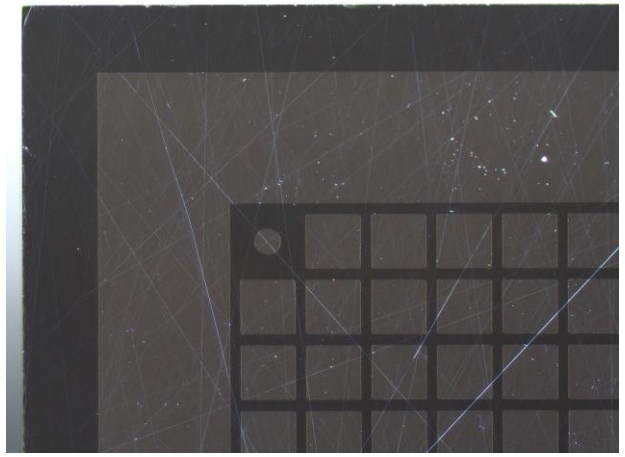

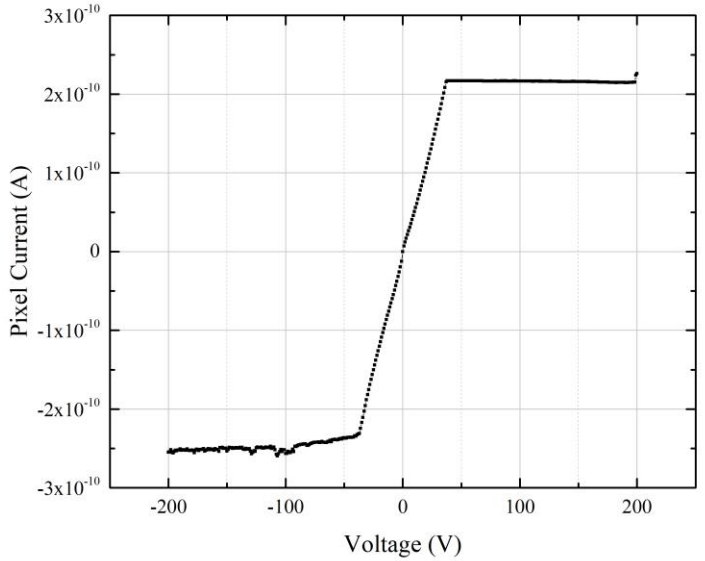

Brookhaven National Laboratory

Acknowledgements

NSLS II Detector Group: D.P. Siddons, A.J. Kuczewski, S. LaMarra, and J. Li.

Instrumentation Division: G. Gaicomini, W. Chen, G. Carini, A. Bolotnikov, E. Muller, G. Deptuch, R. Angona, D. Elliott, D. Pinelli, J. Pinz, A. Verderosa, F. Capocasa, G. Pinaroli, B. Weldon, I. Harding

FZ-Julich : T. Krings

Cornell: S. Gruner, M. Tate, J. Thom-Levy

Stony Brook U/ Weill Cornell: A. Goldan, Z. Han, A. Mukherjee

High-Z Collaboration: Cornell, APS, SLAC, Northwestern